High Clonality of Virus-Specific T Lymphocytes Defined by TCR Usage in the Brains of Mice Infected with West Nile Virus

Kazutaka Kitaura,*,†,‡ Yoshiki Fujii,*,† Daisuke Hayasaka,§ Takaji Matsutani,¶ Kenji Shirai,*,†,‡ Noriyo Nagata,‖ Chang-Kweng Lim,† Satsuki Suzuki,# Tomohiko Takasaki,† Ryuji Suzuki,* and Ichiro Kurane†,‡

It has been reported that brain-infiltrating T lymphocytes play critical roles in the clearance of West Nile virus (WNV) from the brains of mice. We characterized brain-infiltrating T lymphocytes by analyzing the TCR α- and β-chain repertoires, T cell clonality, and CDR3 sequences. CD3$^+$CD8$^+$ T cells were localized in the WNV-infected brains. The expression of CD3, CD8, CD25, CD69, perforin, and granzymes positively correlated with viral RNA levels, and high levels of expression of IFN-γ, TNF-α, and IL-2 were detected in the brains, suggesting that Th1-like cytotoxic CD8$^+$ T cells are expanded in the brains in response to WNV infection. The brain-infiltrating T lymphocytes dominantly used TCR genes, VA1-1, VA2-1, VB5-2, and VB8-2, and exhibited a highly oligoclonal TCR repertoire. Interestingly, the brain-infiltrating T lymphocytes had different patterns of TCR repertoire usages among WNV-, Japanese encephalitis virus-, and tick-borne encephalitis virus-infected mice. Moreover, CD8$^+$ T cells isolated from the brains of WNV-infected mice produced IFN-γ and TNF-α after in vitro stimulation with peritoneal cells infected with WNV, but not with Japanese encephalitis virus. The results suggest that the infiltrating CD8$^+$ T cells were WNV-specific, but not cross-reactive among flaviviruses. T cells from the WNV-infected brains exhibited identical or similar CDR3 sequences in TCRα among tested mice, but somewhat diverse sequences in TCRβ. The results indicate that WNV-specific CD3$^+$CD8$^+$ T cells expanding in the infected brains are highly oligoclonal, and they suggest that TCR α-chains play a dominant and critical role in Ag specificity of WNV-specific T cells. *The Journal of Immunology*, 2011, 187: 000–000.

West Nile virus (WNV) is a member of the Flaviviridae family and causes a range of illnesses from mild fever to acute flaccid paralysis and lethal encephalitis in humans. Approximately 20–30% of infected individuals develop flu-like clinical manifestations characterized as West Nile fever, and about 1 in 150 cases is accompanied by severe neurologic disease, such as cognitive dysfunction, ocular manifestations, meningitis, encephalitis, and flaccid paralysis (1–3). West Nile fever was endemic in the Middle East, Europe, and Africa before the mid-1990s, but has since spread throughout the world, including the Americas (4). However, vaccines or specific therapies for WNV are unavailable for humans. Moreover, the pathogenesis of WNV encephalitis is not clear, especially the reasons why most of the symptomatic cases demonstrate acute febrile illness but some develop severe encephalitis.

CD8$^+$ cytotoxic T cells play essential roles in controlling WNV infection (5) and protection against WNV encephalitis (6). Previously, we have demonstrated the existence of Ag-specific T cells in the brains of C3H mice infected with Japanese encephalitis virus (JEV), which is closely related to WNV (7). In mice infected with flaviviruses, Ag-specific T lymphocytes infiltrating into the CNS mediate the clearance of virus, preventing encephalitis. However, little information regarding Ag specificity and diversity of the CNS-infiltrating T cells is available. Immune responses against virus infections are initiated by specific recognition of a viral Ag presented on an MHC by a TCR. Functional TCR α- and β-chains genes are generated by somatic gene rearrangements of germline-encoded V(D)J and constant gene segments. The Ag specificity and diversity of the TCR depends mainly on CDR3, formed by nucleotide addition/insertion during the gene rearrangements (8) that contact directly with an Ag peptide on MHC (9). Many investigations with quantitative and qualitative analyses of TCR repertoires and CDR3 sequences have contributed to the elucidation of pathological conditions and/or immunological dynamics in infectious disease research (7), pathogenesis of autoimmune diseases (10–12), and/or physiological analysis (13, 14). Additionally, neutralizing Abs induced by WNV partially protect against JEV infection (15). The immunological cross-reaction between closely related flaviviruses raised the question of whether

*Department of Rheumatology and Clinical Immunology, Clinical Research Center for Allergy and Rheumatology, Sagamihara National Hospital, National Hospital Organization, Kanagawa 228-0815, Japan; †Department of Virology 1, National Institute of Infectious Diseases, Tokyo 162-8640, Japan; ‡Department of Infection Biology, Institute of Basic Medical Sciences, University of Tsukuba, Ibaraki 305-8575, Japan; §Department of Virology, Institute of Tropical Medicine, Nagasaki University, Nagasaki 852-8523, Japan; ¶Laboratory of Immune Regulation, Wakayama Medical University, Osaka, 567-0085, Japan; ‖Department of Pathology, National Institute of Infectious Diseases, Tokyo 208-0011, Japan; and #Section of Biological Science, Research Center for Odontology, Nippon Dental University School of Life Dentistry at Tokyo, Tokyo 102-8159, Japan

Address correspondence and reprint requests to Dr. Ichiro Kurane, Department of Virology 1, National Institute of Infectious Diseases, 1-23-1 Toyama, Shinjuku-ku, Tokyo 162-8640, Japan. E-mail address: kurane@nih.go.jp

brain-infiltrating T lymphocytes use identical or similar TCR repertoires among these closely related flaviviruses.

To characterize the brain-infiltrating T lymphocytes in WNV-infected mice, we performed immunohistochemical (IHC) and quantitative real-time RT-PCR (qPCR) analyses for T cell-related surface molecules, cytokines, chemokines, and cytotoxic granules. The results demonstrated that Th1-like cytotoxic CD8$^+$ T cells accumulated in the brains. Next, to disclose Ag specificity and diversity in the brain-infiltrating T lymphocytes, we analyzed the TCR repertoires and TCR clonotypes in the brains of mice infected with WNV, JEV, and tick-borne encephalitis virus (TBEV). The results indicated that T cells accumulated in the mice brains had a distinct TCR repertoire among WNV, JEV, and TBEV and exhibited high oligoclonality. Furthermore, we performed in vitro stimulation assays by coculturing T cells isolated from WNV-infected mouse brains with peritoneal cells (PECs) obtained from different strains of mice that were infected with either WNV or JEV. These T cells produced IFN-γ and TNF-α in response to WNV-infected PECs with a syngeneic MHC haplotype. The present study provides important information about the Ag specificity and diversity of brain-infiltrating T lymphocytes in flavivirus-infected mice.

Materials and Methods
Virus

The NY99-6922 strain of WNV (GenBank accession no. AB185915; http://www.ncbi.nlm.nih.gov/genbank and the JaTH160 strain of JEV (GenBank accession no. AB269326) were used in this study. The WNV was prepared from the conditioned medium of Vero cells that were infected with a previously prepared virus stock (15). Vero cells were maintained in Eagle's MEM (Nissui Pharmaceutical, Tokyo, Japan) containing 10% FCS. The virus titer was 1.4×10^5 PFU/ml. JEV was prepared as described previously (7) with a virus titer of 1×10^{10} PFU/ml. The experiments using live viruses were performed in a biosafety level (BSL) 3 laboratory of the National Institute of Infectious Diseases, Japan, according to standard BSL3 guidelines. The Oshima 5-10 strain of TBEV (GenBank accession no. AB062063) (16) was also used in this study. The virus was prepared from the conditioned medium of baby hamster kidney cells infected with a previously prepared virus stock (17). Baby hamster kidney cells were maintained in Eagle's MEM containing 8% FCS. Experiments using live TBEV were performed in a BSL3 laboratory of the Tokyo Metropolitan Institute for Neuroscience according to standard BSL3 guidelines.

Mice

C3H/HeNJcl (H-2^k), C57BL/6JJcl (H-2^b), and BALB/cAJcl (H-2^d) female mice were purchased from CLEA Japan (Tokyo, Japan) and kept in a specific pathogen-free environment. All animal experiments were done according to the relevant ethical requirements and with approval from the committees for animal experiments at the National Institute of Infectious Diseases and the Tokyo Metropolitan Institute for Neuroscience, Japan.

Virus challenges

Seven-week-old C3H/HeNJcl female mice were injected i.p. with the 30 × LD$_{50}$ (1.3×10^3 PFU/0.5 ml) WNV and the 100 × LD$_{50}$ (1.2×10^4 PFU/0.5 ml) JEV or PBS alone (mock infection). Four, 7, and 10 days later, WNV-infected mice were sacrificed under general anesthesia. Ten days later, JEV-infected mice were sacrificed under general anesthesia. In TBEV

infection, 7-wk-old C3H/HeNJcl female mice were injected s.c. with 1.0×10^3 PFU/0.5 ml TBEV or PBS. Thirteen days later, mice were sacrificed under general anesthesia.

Histological and IHC analyses

Brains were excised for use in histological and IHC examinations. Tissue samples were fixed overnight at 4°C with paraformaldehyde-lysine-periodate, washed with PBS, and immersed in 5% sucrose/PBS for 1 h, in 15% sucrose/PBS for 3 h, and in 30% sucrose/PBS overnight at 4°C. Samples were embedded in Tissu Mount (Chiba Medical, Saitama, Japan) and quick-frozen in a mixture of acetone and dry ice. For histochemical staining, 6-μm cryosections were air-dried on poly-L-lysine–coated glass slides and were stained with H&E. For IHC analyses, cryosections were stained with anti-mouse CD3ε (145-2C11; BD Pharmingen, San Diego, CA), CD4 (GK5.1; BD Pharmingen), and CD8α (53-6.7; BD Pharmingen) mAbs. In short, glass slides were overlaid with PBS containing blocking reagents (a 1:20 dilution of normal goat serum or normal rabbit serum, 0.025% Triton X-100 [Wako Pure Chemicals, Osaka, Japan], and 5% BSA [Sigma-Aldrich, St. Louis, MO]) and incubated for 30 min at room temperature. The mAbs were loaded onto the glass slides and incubated for 1 h at room temperature. After washing with PBS (three times for 5 min), each section was treated with a secondary Ab (biotinylated goat anti-hamster IgG Ab or biotinylated rabbit anti-rat IgG Ab) at room temperature for 1 h and then with avidin–biotin complex for 30 min, followed by 3,3′-diaminobenzidine staining (0.06% 3,3′-diaminobenzidine, 0.03% H_2O_2 in 0.1 M Tris-HCl buffer [pH 7.6]; Wako Pure Chemicals). Finally, the glass slides were counterstained with hematoxylin to visualize nuclei.

Isolation of total RNA from tissues

Fresh brains and spleens infected with WNV or TBEV were excised intact and immediately submerged in RNAlater RNA stabilization reagent (Qiagen, Hilden, Germany) (18). Total RNA was isolated using the RNeasy Lipid Tissue Mini Kit (Qiagen) according to the manufacturer's instructions.

Quantitative estimation of the expression of immune-related genes and WNV RNA in brains and spleens

Expression levels of mRNA for immune-related genes including T cell-related CD Ags, cytokines, chemokines, chemokine receptors, and cytotoxic granules were measured by qPCR using a LightCycler apparatus (Roche Diagnostics, Basel, Switzerland). Previously demonstrated primer pairs specific for GAPDH, CD3, CD4, CD8, IFN-γ, TNF-α, IL-2, IL-4, IL-5, CCL5, CXCL10, and CXCR3 were used in this study (7, 19). Other primer pairs (CCR5, perforin, granzyme A, granzyme B, CD25 [IL-2Rα], and CD69) were designed for this study (Table I). IL-10-specific primers were purchased from Takara Bio (Otsu, Japan). Freshly isolated RNA from the spleens and brains of WNV- or mock-infected mice ($n = 5$) was converted to cDNA using a PrimeScript RT reagent kit (Takara Bio) according to the manufacturer's instructions. The PCR reaction was performed using SYBR Premix TaqII (Takara Bio) for SYBR Green I and was carried out in a 20-μl volume containing 2 μl cDNA template originating from 50 ng total RNA, 0.4 μl each 10 μM forward and reverse primers, and 10 μl SYBR Premix TaqII. After an initial denaturation step at 95°C for 10 s, temperature cycling was initiated. Each cycle consisted of 95°C for 5 s and 60°C for 30 s, and the fluorescence was read at the end of this second step. In total, 40 cycles for GAPDH and 50 cycles for other primer sets were performed accordingly. Melting curve analysis was performed immediately after amplification at a linear temperature transition rate of 0.1°C/s from 65°C to 95°C with continuous fluorescence acquisition. The absolute copy number of each gene was calculated by using a standard curve generated by serial dilution of the recombinant plasmid DNA encoding gene of interest, ranging from 10^1 to 10^8 copies. Calculated copy numbers were normalized based on the copy numbers of the housekeeping gene GAPDH.

Table I. Sequences of qPCR primers

Targets	Forward Primer (5′–3′)	Reverse Primer (5′–3′)
CCR5	ATATGCAAAGGGACGGACAC	GCAAGAAGCGACTTTATGGC
IL-10	GACCAGCTGGACAACATACTGCTAA	GATAAGGCTTGGCAACCCAAGTAA
Perforin	GCCTGGTACAAAAACCTCCA	AGGGCTGTAAGGACCGAGAT
Granzyme A	CCTGAAGGAGGCTGTGAAAG	GAGTGAGCCCCAAGAATGAA
Granzyme B	CCATCGTCCCTAGAGCTGAG	TTGTGGAGAGGGCAAACTTC
CD25	AAGATGAAGTGTGGGAAAACGG	GGGAAGTCTGTGGTGGTTATGG
CD69	AGGATCCATTCAAGTTTCTATCCC	CAACATGGTGGTCAGATGATTCC

The viral RNA levels of WNV were examined with envelope-specific forward and reverse primers (5'-TCAGCGATCTCTCCACCAAAG-3' and 5'-GGGTCAGCACGTTTGTCATTG-3') and a dual fluorophore-labeled probe (5'-CFSE-TGCCCGACCATGGGAGAAGCTC-TAMRA-3') using a Prism 7000 sequence detection system (Applied Biosystems, Foster, CA). A TaqMan Ez RT-PCR kit (Applied Biosystems) was used according to the manufacturer's instructions. A total reaction mixture of 25 μl containing 50 ng total RNA was incubated at 48°C for 30 min for reverse transcription and then at 95°C for 10 min for inactivation of reverse transcriptase and initial denaturation. PCR was carried out for 40 cycles at 95°C for 15 s and 57°C for 1 min, and the fluorescence was read at the final PCR round. The copy number of each sample was determined on the basis of a standard curve created with a serial dilution of in vitro-synthesized WNV RNA ranging from 10^1 to 10^8 copies, provided by Dr. Soichi Nukuzuma (Kobe Institute of Health, Kobe, Hyogo, Japan).

TCR repertoire analysis

TCR repertoire analysis was performed with WNV- and TBEV-infected mice samples ($n = 5$) by an adaptor ligation-mediated PCR and microplate hybridization assay method (20–22). Briefly, isolated total RNA was converted to double-stranded cDNA using a SuperScript cDNA synthesis kit (Invitrogen, Carlsbad, CA) according to the manufacturer's instructions, except that a specific primer (BSL-18E) was used (22). The P10EA/P20EA adaptors were ligated to the 5' end of the cDNA and this adaptor-ligated cDNA was cut with SphI. PCR was performed with TCR α-chain C region-specific (MCA) 1 or TCR β-chain C region-specific primers (MCB) 1 and P20EA. The second PCR was performed with MCA2 or MCB2 and P20EA. The third PCR was performed using both P20EA and 5'-biotinylated MCA3 or MCB3 primer for biotinylation of PCR products.

Ten picomoles of amino-modified oligonucleotides specific for the TCR α-chain variable (TCRAV) and TCR β-chain variable (TCRBV) segments were immobilized onto carboxylate-modified 96-well microplates with water-soluble carbodiimide. Prehybridization and hybridization were performed in GMCF buffer (0.5 M Na_2HPO_4 [pH 7.0], 1 mM EDTA, 7% SDS, 1% BSA, and 7.5% formamide) at 47°C. One hundred microliters of the denatured 5'-biotinylated PCR products was mixed with the equivalent volume of 0.4 N NaOH/10 mM EDTA, and the mixture was added to 10 ml GMCF buffer. One hundred microliters of hybridization solution was used in each well of the microplate containing immobilized oligonucleotide probes specific for V segments. After hybridization, wells were washed four times with washing buffer (2× SSC, 0.1% SDS) at room temperature. Plates were then incubated at 37°C for 10 min for stringency washing. After washing four times with the same washing buffer, 200 μl TB-TBS buffer (10 mM Tris-HCl, 0.5 M NaCl [pH 7.4], 0.5% Tween 20, and 0.5% blocking reagent; Roche Diagnostics) was added to block nonspecific binding. Next, 100 μl 1:2000 diluted alkaline phosphatase-conjugated streptavidin in TB-TBS was added, and the sample was incubated at 37°C for 30 min. Plates were washed six times in T-TBS (10 mM Tris-HCl, 0.5 M NaCl [pH 7.4], 0.5% Tween 20). For color development, 100 μl substrate solution (4 mg/ml p-nitrophenylphosphate [Sigma Aldrich] in 10% diethanolamine [pH 9.8]) was added, and absorbance was determined at 405 nm. The ratio of the hybridization intensity of each TCR V region (TCRV)-specific probe to that of a TCR C region-specific probe (V/C value) was determined using the TCR cDNA concentrated samples that contained the corresponding TCRV segment and the universal TCR constant segment, respectively. Absorbance obtained with each TCRV-specific probe was divided by the corresponding V/C value. The relative frequency was calculated based on the corrected absorbances using the formula: relative frequency (%) = (corrected absorbance of TCRV-specific probe/ sum of corrected absorbances of TCRV-specific probes) × 100.

T cell clonality analysis with CDR3 size spectratyping

The level of T cell clonality was evaluated in samples from WNV- and TBEV-infected mice ($n = 5$) using a CDR3 size spectratyping method (23). PCR was performed for 30 cycles in a 20 μl volume under the same conditions as described above. The PCR mixture consisted of 1 μl 1:20 or 1:50 diluted second PCR product, 0.1 μM 5'-Cy5 MCA3/MCB3 primer, and 0.1 μM primer specific for each variable segment. Two microliters 1:20 diluted PCR product was analyzed with the CEQ8000 genetic analysis system (Beckman Coulter, Fullerton, CA). The spleens of mock-infected mice were used as normal controls showing a Gaussian distribution pattern with multiple peaks.

Determination of CDR3 nucleotide sequences

PCR was performed with 1 μl 1:20 diluted second PCR product, using a forward primer specific for the V region and a reverse primer specific for

the C region (MCA4 or MCB4) under the conditions described above. The primers used in this study were as follows: VA1-1, 5'-AGACTCCCAGC-CCAGTGACT-3'; VA2-1, 5'-TGCAGTTATGAGGACAGCACTT-3'; VB5-2, 5'-GGATTCCTACCCAGCAGATTC-3'; and VB8-2, 5'-GGCTACC-CCCTCTCAGACAT-3'. After elution from agarose gels, PCR products were cloned into the pGEM-T Easy Vector (Promega, Madison, WI). The recombinant plasmid DNA was transfected into DH5α competent cells. Sequence reactions were performed with the GenomeLab DTCS Quick Start Kit (Beckman Coulter) and analyzed by the CEQ8000 genetic analysis system (Beckman Coulter). In total, 64 clones from each sample of WNV- and TBEV-infected mouse brains ($n = 5$) were examined in this experiment.

In vitro stimulation of T cells from WNV-infected mouse brain

WNV- or JEV-infected C3H/HeN mice ($n = 8$) were sacrificed under general anesthesia on day 10 postinfection, and brains were removed. Brains were kept on ice in RPMI 1640 containing 10% FCS and homogenized gently by pressing through a 100-μm mesh tissue strainer (BD Pharmingen). Homogenates were then centrifuged at 400 × g for 10 min, and cell pellets were resuspended in 5 ml RPMI 1640 and layered over 5 ml Lympholyte-M (Cedarlane Laboratories, Hornby, ON, Canada) before centrifugation at 1000 × g for 20 min at 22°C. Next, the isolated lymphocyte pool was washed twice and resuspended in MACS buffer (Ca^+- and Mg^+-free PBS, 2 mM EDTA, and 0.5% BSA) and incubated with anti-CD4 and/or anti-CD8 MACS beads (Miltenyi Biotec, Auburn, CA) at 4°C for 15 min. Cell suspensions were diluted 20 times in
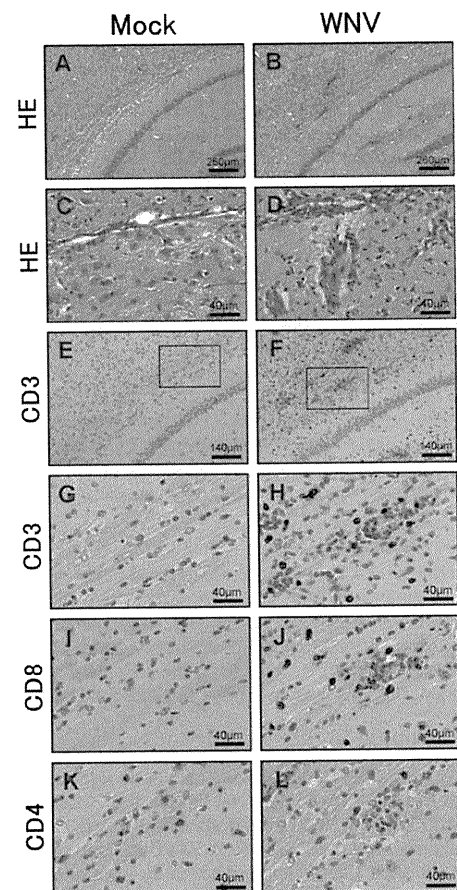
FIGURE 1. Histopathological study and IHC analysis of CD3^{+}, CD8^{+}, and CD4^{+} cells in WNV-infected mouse brain. Representative photomicrographs of brain sections from mock-infected or WNV-infected mice at day 10 postinfection, stained with H&E (*A–D*) and CD3, CD4, and CD8 (*E–L*). Neuronal degeneration and inflammatory cell infiltration in hippocampus and perivascular areas are shown in WNV-infected mouse brains, but not those of mock-infected mice. For the IHC analysis, the localization of CD3^{+} and CD8^{+} cells is shown throughout the brain of WNV-infected mice, but not those of mock-infected mice (*E–J*). Alternatively, CD4^{+} cells were detected sporadically in both WNV- and mock-infected mice (*K, L*). The area of higher magnifications (original magnification ×3.5) are indicated by the black boxes in *E* and *F*.

MACS buffer and centrifuged at 300 × g for 10 min. Cell pellets were resuspended in MACS buffer and filtered through MACS LS separation columns (Miltenyi Biotec), according to the manufacturer's protocol. Collected CD4^{+} and/or CD8^{+} cells were resuspended in RPMI 1640 containing 10% FCS and antibiotics (assay medium), adjusted to 2.5×10^6 cells/ml, and were used in in vitro stimulation assays. PECs were collected in 10 ml cold Ca^{+}- and Mg^{+}-free PBS, from C3H/HeN, C57BL/6j, and BALB/c mice ($n = 3$) after scarifying the mice under general anesthesia. The cells were centrifuged at 600 × g for 5 min, resuspended in assay medium, and counted. After infection with WNV or JEV at a multiplicity

of infection of 100 PFU/cell at 37°C in 5% CO_2 for 60 min, the cells were washed twice with assay medium. The concentration of PECs was adjusted to 5.0×10^5 cells/ml, and 100 μl PEC was dispensed into flat-bottom 96-well trays (Nunc, Roskilde, Denmark). Subsequently, 100 μl 2.5×10^5 T cells from WNV- or JEV-infected C3H mouse brains was added and cultured at 37°C in 5% CO_2 for 12 h. Culture supernatant fluids were collected, and levels of IFN-γ and TNF-α were measured by ELISA (MIF00 and MTA00, respectively; R&D Systems, Minneapolis, MN) according to the manufacturer's instructions. Cells were then further cultured for 3 d and used for CDR3 analysis.
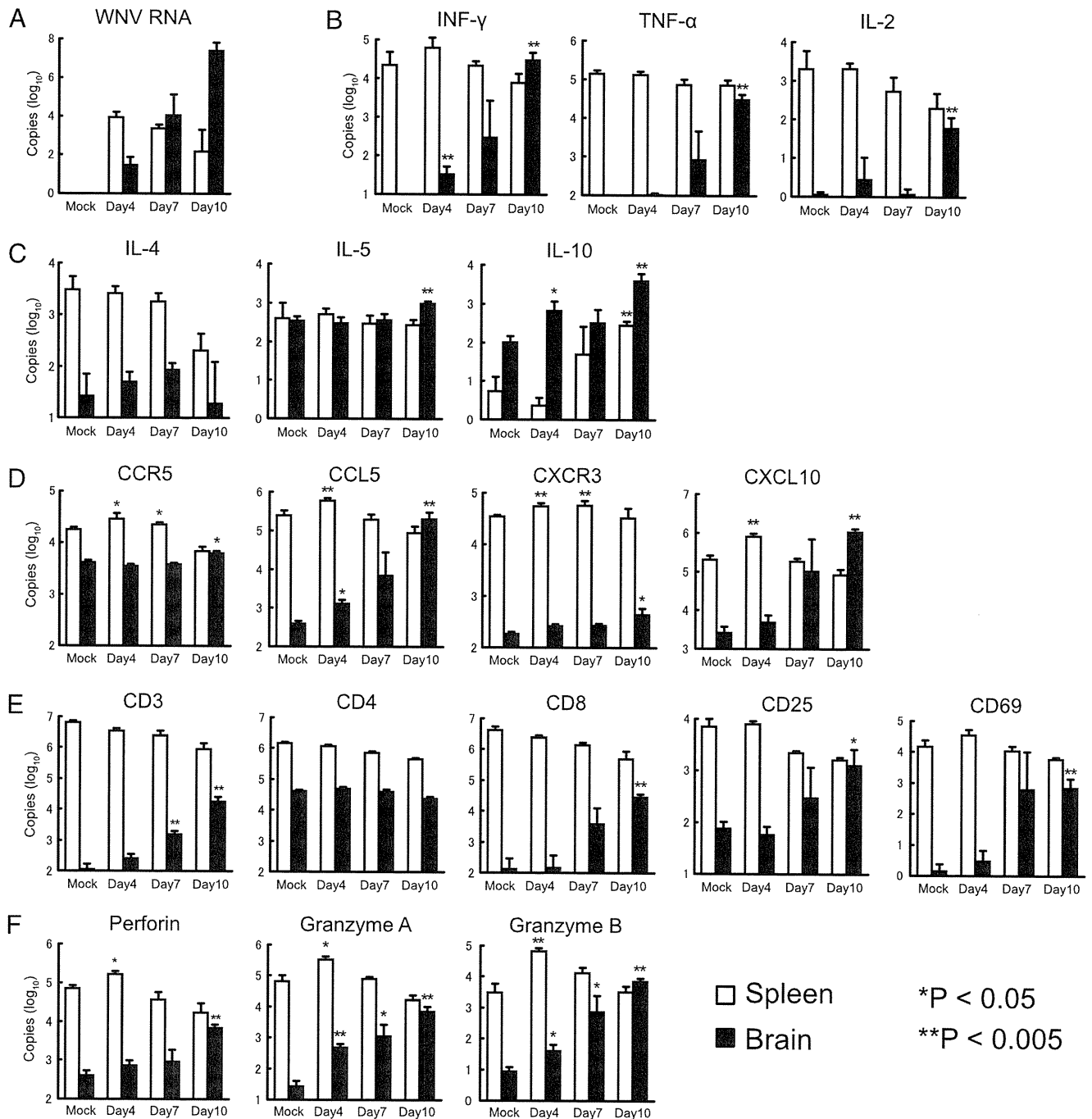
FIGURE 2. Quantification of WNV RNA and of T cell immune-related gene mRNAs by qPCR. Copy number of WNV RNA (*A*), the mRNA expression level of IFN-γ, TNF-α, and IL-2 as Th1-type cytokines (*B*), IL-4, IL-5, and IL-10 as Th2 type cytokines (*C*), CCR5, CCL5, CXCR3, and CXCL10 as chemokines and chemokine receptors (*D*), CD3, CD4, CD8, CD25 (IL-2R), and CD69 as T cell–related Ags (*E*), and perforin, granzyme A, and granzyme B as cytotoxic granules (*F*) are shown. The copy numbers per 50 ng total RNA were calibrated with GAPDH expression, except that WNV RNA was calculated from the standard density of in vitro-synthesized WNV RNA. RNA was extracted from spleens (open bars) or brains (filled bars) of mock-infected mice (Mock) or WNV-infected mice at 4, 7, and 10 d after virus inoculation. Open or filled bars and vertical error bars indicate mean ± SD of five mice. Significant differences are shown when compared with mock spleen or brain using a Student unpaired *t* test (*$p < 0.05$, **$p < 0.005$). All experiments were performed in triplicate.

Statistical analysis

Differences were statistically analyzed by a Student unpaired t test using StatView 5.0 for Windows (SAS Institute, Cary, NC). A p value <0.05 was determined to be statistically significant. Moreover, to assess biologically significant differences, a 5% cut-off threshold was added for TCR repertoires.

Results

Histopathological study of brains from WNV-infected mice

Brains were removed from WNV- or mock-infected mice 10 d postinfection and prepared for histopathological examinations as described in *Materials and Methods*. Representative histological changes are shown in Fig. 1A–D. Severe neuronal degeneration and inflammatory cell infiltration were detected in the brains from infected mice, especially in the hippocampus, perivascular tissue, and cerebral meninges. In WNV-infected mouse brains, but not in mock-infected mouse brains, CD3$^+$ and CD8$^+$ T cells were also widely detected, especially in the cerebral meninges, perivascular tissue, and hippocampus (Fig. 1E–J). CD4$^+$ cells were detected in brain sections both from WNV- and mock-infected mice (Fig. 1K, 1L).

Propagation of WNV and cytokine expression in brains from WNV-infected mice

The amount of WNV RNA in brains and spleens was measured by qPCR after i.p. inoculation of the virus (Fig. 2A). WNV RNA was first detected on day 4 in both organs. RNA levels increased largely with time in the brains, whereas they gradually decreased after day 4 in the spleens. Cytokine expression in the brains of WNV-infected mice was also measured (Fig. 2B, 2C). A temporal increase in the expression of IFN-γ, TNF-α, and IL-2 was detected in the brains of the WNV-infected mice, but not in those of mock-infected ones. IL-4, IL-5, and IL-10 expression was detected in the brains of mock-infected mice. The expression levels of IL-5 increased significantly on day 10 in WNV-infected mice. The expression of IL-10 increased on day 4 in the brains and slowly in the spleens following WNV infection. The expression levels of chemokines (CCL5 and CXCL10) and chemokine receptors (CCR5 and CXCR3) considerably increased in the brains after WNV infection (Fig. 2D). In particular, the expression levels of CCL5 and CXCL10 were increased >100-fold on day 10 compared with day 4. These results indicated that expression
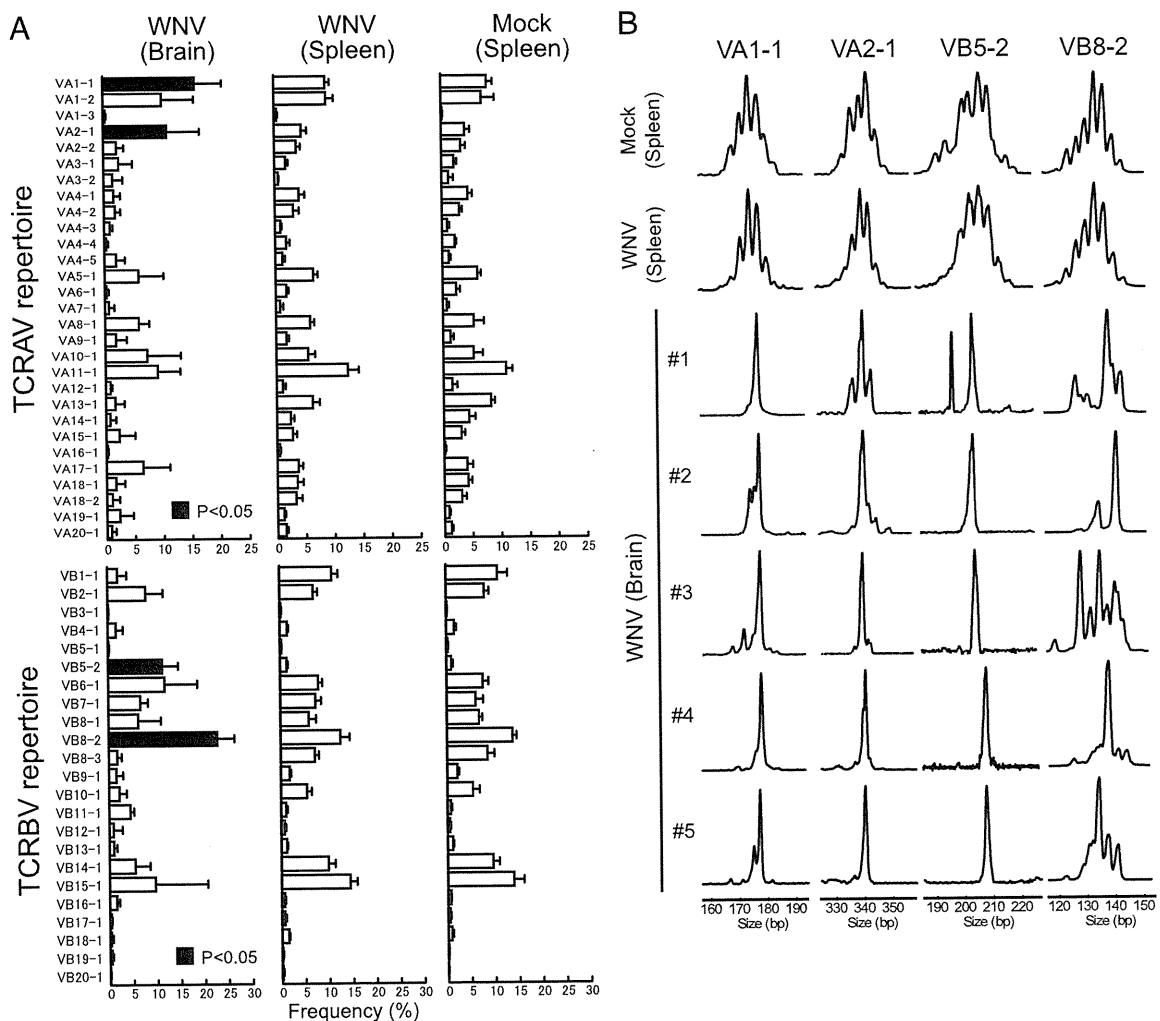
FIGURE 3. TCR repertoire analysis and CDR3 size spectratyping in spleens and brains of WNV-infected mice. *A*, TCRAV and TCRBV repertoires were analyzed by microplate hybridization assay method. The open or filled bars and horizontal bars indicate mean ± SD of frequencies in five mice. In the brains of WNV-infected mice on day 10, percentage frequencies of T cells bearing VA1-1, VA2-1, VB5-2, and VB8-2 were significantly increased compared with those of mock-infected mouse spleens ($p < 0.05$, Student unpaired t test, filled bars). All experiments were performed in triplicates. *B*, CDR3 size spectratyping patterns of VA1-1, VA2-1, VB5-2, and VB8-2 in five mice infected with WNV on day 10. Multiple peaks with a Gaussian distribution showing the presence of polyclonal T cells are seen in the spleen of mock-infected mice (control). The same pattern was found in the spleens of WNV-infected mice. In contrast, a single or a few peaks, signifying high levels of oligoclonality, were obtained from all VA and VB families tested in the WNV-infected brains.

levels of Th1-type cytokines and chemokines positively correlated with the propagation of WNV in the brains.

Infiltration of T cells in the brains of WNV-infected mice

To confirm the presence of brain-infiltrating T cells, expression of CD3, CD4, CD8, CD25, and CD69 was measured (Fig. 2E). CD3 and CD8 were expressed at low levels during the early phase of infection in WNV- and mock-infected brains. However, their expression considerably increased during the late phase of infection. CD25 and CD69 showed a similar expression pattern as CD3 and CD8. These results suggested that activated CD3$^+$CD8$^+$ T cells infiltrated the brains of the WNV-infected mice. CD4 transcripts were consistently detected in both WNV- and mock-infected mice. The expression of cytotoxic granule components (perforin, granzyme A, and granzyme B) was measured by qPCR (Fig. 2F) and found to be rapidly increased in the early stages of WNV infection in both spleens and brains, positively correlating with CD3, CD8, CD25, and CD69 expression. These results suggested that cytotoxic T lymphocytes expanded in the brains of WNV-infected mice.

TCR repertoire and clonality in brain-infiltrating T cells

TCRAV and TCRBV repertoires were analyzed from the spleens and brains of WNV- or mock-infected mice 10 d postinfection (Fig. 3A). The TCRAV and TCRBV repertoires were not significantly different in the spleens between the WNV- and the mock-infected mice. In contrast, the percentage frequencies of T cells bearing VA1-1, VA2-1, VB5-2, and VB8-2 were significantly higher in the brains of WNV-infected mice than in the spleens from WNV- or mock-infected mice. The expression levels of these families were increased from day 4 to day 10 in the brains (Fig. 4A). Expression of TCR genes was not detected in the brains from mock-infected

mice. Furthermore, T cell clonality was examined by a CDR3 size spectratyping method and a significant increase in the clonality was detected in VA1-1, VA2-1, VB5-2, and VB8-2 (Fig. 3B). Polyclonal peak patterns were detected in the spleens of mock- and WNV-infected mice while oligoclonal or monoclonal peak patterns were detected in the brains of WNV-infected mice on day 10. Dominant peaks in VA1-1, VA2-1, and VB5-2 appeared to be identical in size among individual mice, whereas an oligoclonal peak pattern was detected in VB8-2.

Determination of CDR3 nucleotide sequences

CDR3 nucleotide sequences were determined with cDNA clones obtained from the spleen of mock-infected mice and the brains of WNV-infected mice. Predicted amino acid sequences with occurrence frequencies of the respective cDNA clones are shown in Fig 5. The cDNA clones obtained from the spleen of the mock-infected mice displayed highly diverse CDR3 sequences (data not shown), which corresponded to the results from CDR3 size spectratyping. In contrast, oligoclonal or monoclonal T cells were detected in VA1-1, VA2-1, and VB5-2 in the brains of WNV-infected mice.

In VA1-1, five clonotypes (CAVS-IG-NSGTYQRFG, CAVS-MG-NSGTYQRFG, CAVS-KG-NSGTYQRFG, CAVS-PG-NSG-TYQRFG, and CAVS-MG-GYQNFYFG) were obtained from the brains of different mice (Fig. 5A). Interestingly, these clonotypes had only one amino acid difference in the N region. Additionally, preferential usage in AJ13 was observed in the WNV-infected brains (47 of 51 clones for mouse 1, 47 of 52 for mouse 2, 20 of 50 for mouse 3, 15 of 52 for mouse 4, and 25 of 51 for mouse 5). A similar result was also obtained from sequence analysis of VA2-1 (Fig. 5B). Two dominant clonotypes (CAAS-EG-GNYK-

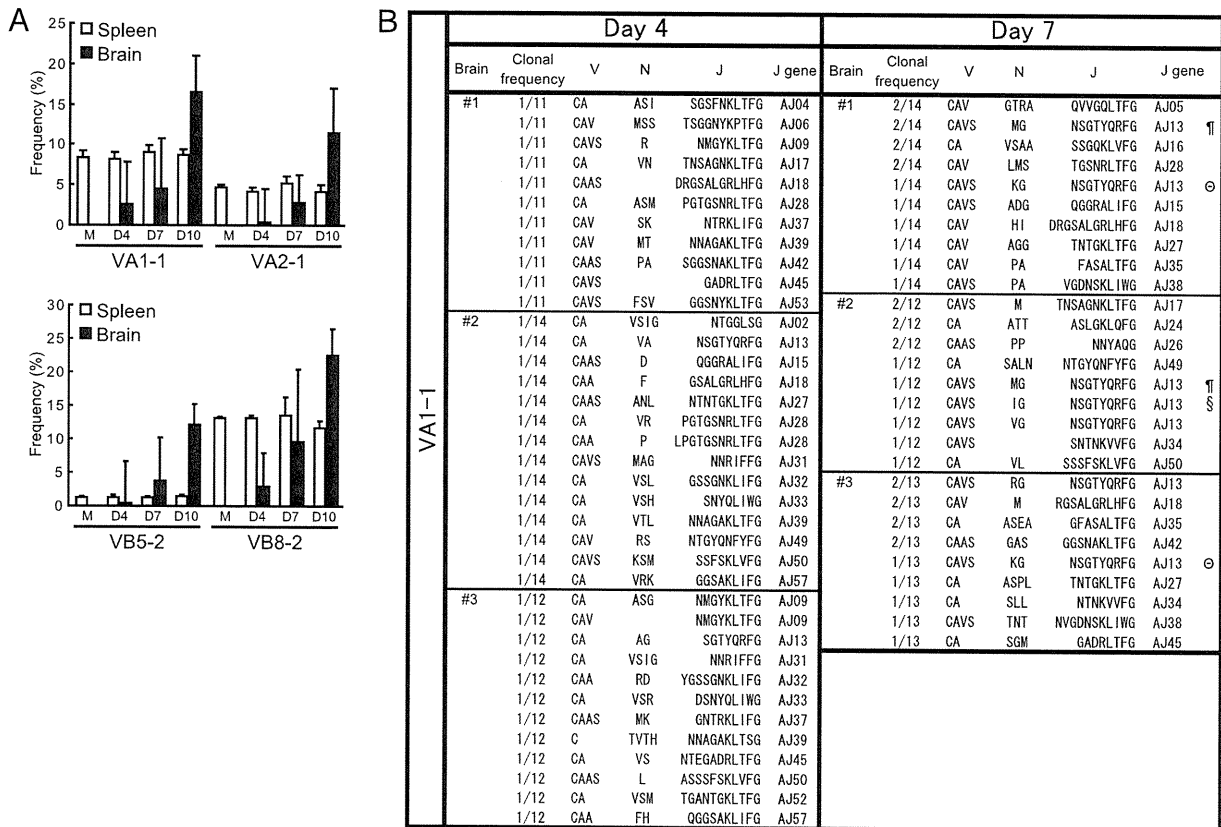| Brain	Clonal frequency	V	N	J	J gene	Brain	Clonal frequency	V	N	J	J gene
#1	1/11	CA	ASI	SGSFNKLTFG	AJ04	#1	2/14	CAV	GTRA	QVVGQLTFG	AJ05
	1/11	CAV	MSS	TSGGNYKPTFG	AJ06		2/14	CAVS	MG	NSGTYQRFG	AJ13 ¶
	1/11	CAVS	R	NMGYKLTFG	AJ09		2/14	CA	VSAA	SSGQKLVFG	AJ16
	1/11	CA	VN	TNSAGNKLTFG	AJ17		2/14	CAV	LMS	TGSNRLTFG	AJ28
	1/11	CAAS		DRGSALGRLHFG	AJ18		1/14	CAVS	KG	NSGTYQRFG	AJ13 ⊖
	1/11	CA	ASM	PGTGSNRLTFG	AJ28		1/14	CAVS	ADG	QGGRALIFG	AJ15
	1/11	CAV	SK	NTRKLIFG	AJ37		1/14	CAV	HI	DRGSALGRLHFG	AJ18
	1/11	CAV	MT	NNAGAKLTFG	AJ39		1/14	CAV	AGG	TNTGKLTFG	AJ27
	1/11	CAAS	PA	SGGSNAKLTFG	AJ42		1/14	CAV	PA	FASALTFG	AJ35
	1/11	CAVS		GADRLTFG	AJ45		1/14	CAVS	PA	VGDNSKLIWG	AJ38
	1/11	CAVS	FSV	GGSNYKLTFG	AJ53	#2	2/12	CAVS	M	TNSAGNKLTFG	AJ17
#2	1/14	CA	VSIG	NTGGLSG	AJ02		2/12	CA	ATT	ASLGKLQFG	AJ24
	1/14	CA	VA	NSGTYQRFG	AJ13		2/12	CAAS	PP	NNYAQG	AJ26
	1/14	CAAS	D	QGGRALIFG	AJ15		1/12	CA	SALN	NTGYQNFYFG	AJ49
	1/14	CAA	F	GSALGRLHFG	AJ18		1/12	CAVS	MG	NSGTYQRFG	AJ13 ¶
	1/14	CAAS	ANL	NTNTGKLTFG	AJ27		1/12	CAVS	IG	NSGTYQRFG	AJ13 §
	1/14	CA	VR	PGTGSNRLTFG	AJ28		1/12	CAVS	VG	NSGTYQRFG	AJ13
	1/14	CAA	P	LPGTGSNRLTFG	AJ28		1/12	CAVS		SNTNKVVFG	AJ34
	1/14	CAVS	MAG	NNRIFFG	AJ31		1/12	CA	VL	SSSFSKLVFG	AJ50
	1/14	CA	VSL	GSSGNKLIFG	AJ32	#3	2/13	CAVS	RG	NSGTYQRFG	AJ13
	1/14	CA	VSH	SNYQLIWG	AJ33		2/13	CAV	M	RGSALGRLHFG	AJ18
	1/14	CA	VTL	NNAGAKLTFG	AJ39		2/13	CA	ASEA	GFASALTFG	AJ35
	1/14	CAV	RS	NTGYQNFYFG	AJ49		2/13	CAAS	GAS	GGSNAKLTFG	AJ42
	1/14	CAVS	KSM	SSFSKLVFG	AJ50		1/13	CAVS	KG	NSGTYQRFG	AJ13 ⊖
	1/14	CA	VRK	GGSAKLIFG	AJ57		1/13	CA	ASPL	TNTGKLTFG	AJ27
#3	1/12	CA	ASG	NMGYKLTFG	AJ09		1/13	CA	SLL	NTNKVVFG	AJ34
	1/12	CAV		NMGYKLTFG	AJ09		1/13	CAVS	TNT	NVGDNSKLIWG	AJ38
	1/12	CA	AG	SGTYQRFG	AJ13		1/13	CA	SGM	GADRLTFG	AJ45
	1/12	CA	VSIG	NNRIFFG	AJ31						
	1/12	CAA	RD	YGSSGNKLIFG	AJ32						
	1/12	CA	VSR	DSNYQLIWG	AJ33						
	1/12	CAAS	MK	GNTRKLIFG	AJ37						
	1/12	C	TVTH	NNAGAKLTSG	AJ39						
	1/12	CA	VS	NTEGADRLTFG	AJ45						
	1/12	CAAS	L	ASSSFSKLVFG	AJ50						
	1/12	CA	VSM	TGANTGKLTFG	AJ52						
	1/12	CAA	FH	QGGSAKLIFG	AJ57						

FIGURE 4. A, Increase in the percentage frequencies of T cells bearing VA1-1, VA2-1, VB5-2, and VB8-2 in WNV-infected mouse brains. B, Amino acid sequences of CDR3 regions of VA1-1 in WNV-infected mouse brains on day 4 and day 7 postinfection. Identical sequences detected in different individual mice are marked by the symbols.

A — VA 1-1

Brain	Clonal frequency	V	N	J	J gene	
#1	24/51	CAVS	IG	NSGTYQRFG	AJ13	§
	21/51	CAVS	MG	NSGTYQRFG	AJ13	¶
	3/51	CA	ASGL	SNTNKVVFG	AJ34	
	2/51	CAVS	KG	NSGTYQRFG	AJ13	Θ
	1/51	CA	AL	NTGYQNFYFG	AJ49	
#2	33/52	CAVS	LA	NSGTYQRFG	AJ13	
	8/52	CAVS	RG	NSGTYQRFG	AJ13	
	6/52	CAVS	MG	NSGTYQRFG	AJ13	¶
	3/52	CAVS	MG	GYQNFYFG	AJ49	†
	1/52	CA	ASME	GDNSKLIWG	AJ38	
	1/52	CA	AED	YANKMICG	AJ47	
#3	13/50	CAVS	PG	NSGTYQRFG	AJ13	‡
	9/50	CA	AN	NVGDNSKLIWG	AJ38	ж
	8/50	CA	ASM	TGNTRKLIFG	AJ37	
	6/50	C	GGKEG	GADRLTFG	AJ45	
	4/50	CAVS	MG	NSGTYQRFG	AJ13	¶
	3/50	CAVS	MG	GYQNFYFG	AJ49	†
	3/50	CAVS	PA	NSGTYQRFG	AJ13	
	2/50	CAV		NTNTGKLTFG	AJ27	
	1/50	C	GGKG	GSALGRLHFG	AJ18	
	1/50	CA	ASI	NTNTGKLTFG	AJ27	
#4	26/52	CAV	RPT	ASLGKLQFG	AJ24	
	15/52	CAVS	IG	NSGTYQRFG	AJ13	§
	6/52	CAVS	RG	QGGRALIFG	AJ15	
	3/52	CAAS	P	SGGSNAKLTFG	AJ42	
	2/52	CA	ASEMD	YANKMICG	AJ47	
#5	18/51	CAVS	KG	NSGTYQRFG	AJ13	Θ
	12/51	CAVS		TNAYKVIFG	AJ30	
	9/51	CAVS	R	TQVVGQLTFG	AJ05	
	7/51	CA	PG	NSGTYQRFG	AJ13	‡
	4/51	CA	AN	NVGDNSKLIWG	AJ38	ж
	1/51	CAV	LTG	GADRLTFG	AJ45	

B — VA 2-1

Brain	Clonal frequency	V	N	J	J gene	
#1	34/50	CAAS	EG	GNYKYVFG	AJ40	§
	6/50	CA	PRG	NNYAQGLTFG	AJ26	
	5/50	CAAS	EG	TNTGKLTFG	AJ27	
	3/50	CAA	VD	YANKMICGLG	AJ47	
	2/50	CAA		TGGNNKLTFG	AJ56	
#2	18/53	CAAS	G	GSALGRLHFG	AJ18	
	15/53	CAAS	VA	GNYKYVFG	AJ40	
	14/53	CAAS	EA	GNYKYVFG	AJ40	¶
	3/53	CAA	NEA	GNYKYVFG	AJ40	
	2/53	CAAS	AVY	NTNTGKLTFG	AJ27	
	1/53	CAAS	VS	SGGNYKPTFG	AJ06	
#3	15/52	CAA	RG	NNYAQGLTFG	AJ26	
	11/52	CAAS	EA	GNYKYVFG	AJ40	¶
	7/52	CAAS	G	NNYAQGLTFG	AJ26	
	6/52	CA	VRG	NNYAQGLTFG	AJ26	
	6/52	CAAS	EG	GNYKYVFG	AJ40	§
	5/52	CAAS	ET	GNYKYVFG	AJ40	
	2/52	CAA	RD	VGDNSKLIWG	AJ38	
#4	21/52	CAAS	EA	GNYKYVFG	AJ40	¶
	14/52	CAAS	P	TNAYKVIFG	AJ30	
	12/52	CAA	I	TGGNNKLTFG	AJ56	
	4/52	CAAS	MA	GNYKYVFG	AJ40	
	1/52	CA	G	NNNAGAKLTFG	AJ39	
#5	17/50	CAAS	EA	GNYKYVFG	AJ40	¶
	11/50	CAAS	LA	GNYKYVFG	AJ40	
	9/50	CAA	RGN	YAQGLTFG	AJ26	
	8/50	CAAS	NA	NAYKVIFG	AJ30	
	3/50	CAAS	AGD	NYAQGLTFG	AJ26	
	2/50	CA	V	NAGAKLTFG	AJ39	

C — VB 5-2

Brain	Clonal frequency	V	N-D-N	J	J gene
#1	49/52	CASS	PGTGG	YEQYFG	BJ2.7
	3/52	CASS	RTG	SAETLYFG	BJ2.3
#2	46/53	CASS	RGD	YAEQFFG	BJ2.1
	5/53	CAS	FRGD	YAEQFFG	BJ2.1
	2/53	CASS	GTGG	NERFFG	BJ1.4
#3	34/51	CASS	LEL	YAEQFFG	BJ2.1
	13/51	CASS	PEL	YAEQFFG	BJ2.1
	4/51	CASS	LDP	EQYFG	BJ2.7
#4	26/51	CASS	PRD	NYAEQFFG	BJ2.1
	15/51	CASS	LGGG	SYEQYFG	BJ2.7
	8/51	CASS	LLDN	AETLYFG	BJ2.3
	2/51	CASS	LTGA	NTEVFFG	BJ1.1
#5	42/51	CASS	LRDS	YAEQFFG	BJ2.1
	9/51	CASS	LNRV	YAEQFFG	BJ2.1

D — VB 8-2

Brain	Clonal frequency	V	N	J	J gene
#1	18/52	CASG	DWGGAQ	SQNTLYFG	BJ2.4
	10/52	CASG	DRTGL	NERLFFG	BJ1.4
	9/52	CASG	DWTGK	SQNTLYFG	BJ2.4
	7/52	CASG	EWGG	AEQFFG	BJ2.1
	3/52	CASG	DVGQG	NTEVFFG	BJ1.1
	3/52	CAS	SATTGG	NSDYTFG	BJ1.2
	2/52	CASG	DDR	YEQYFG	BJ2.7
#2	28/53	CASG	DWAGFS	SYEQYFG	BJ2.7
	9/53	CAS	SDDRG	SAETLYFG	BJ2.3
	9/53	CASG	DPGG	SYEQYFG	BJ2.7
	3/53	CASG	ESGARD	NSPLYFA	BJ1.6
	2/53	CAS	SPGTP	SYEQYFG	BJ2.7
	1/53	CAS	SDGTGDN	NSPLYFA	BJ1.6
	1/53	CASG	ERAGFS	SYEQYFG	BJ2.7
#3	16/50	CASG	DWG	DTQYFG	BJ2.5
	13/50	CASG	DAG	NQDTQYFG	BJ2.5
	8/50	CASG	DAWGR	EQYFG	BJ2.7
	7/50	CASG	DWTGDT	YAEQFFG	BJ2.1
	3/50	CASG	DGGG	EQYFG	BJ2.7
	2/50	CASG	DWTGGAG	QNTLYFG	BJ2.4
	1/50	CASG	DWTGD	NYAEQFFG	BJ2.1
#4	32/51	CASG	GLGS	SAETLYFG	BJ2.3
	8/51	CASG	DWTGGD	ERLFFG	BJ1.4
	5/51	CASG	DAGN	SYEQYFG	BJ2.7
	4/51	CASG	DWTGGALG	QNTLYFG	BJ2.4
	2/51	CASG	DL	YNSPLYFAAG	BJ1.6
#5	16/50	CASG	GTGGL	NTLYFG	BJ2.4
	13/50	CASG	EPGGA	NTLYFG	BJ2.4
	8/50	CASG	DARD	SNERFFG	BJ1.4
	4/50	CAS	RPRDWGN	YEQYFG	BJ2.7
	3/50	CASG	DARTN	SGNTLYFG	BJ1.3
	3/50	CAS	SDWGA	SAETLYFG	BJ2.3
	2/50	CASG	AQGG	ETLYFG	BJ2.3
	1/50	CASG	DEE	NTLYFG	BJ2.4

FIGURE 5. Amino acid sequences of CDR3 regions of VA1-1 (*A*), VA2-1 (*B*), VB5-2 (*C*), and VB8-2 (*D*) in WNV-infected mice brain on day 10. In each family, identical sequences detected in different individual mice are marked by the symbols.

YVFG and CAAS-EA-GNYKYVFG) appeared from the brains of different mice. These clonotypes had similar CDR3 sequences and the common AJ40 segment. Sequence analysis with VB5-2 exhibited extremely high levels of oligoclonality: 49 of 52 clones in mouse 1, 46 of 53 clones in mouse 2, 34 of 51 clones in mouse 3, 26 of 51 clones in mouse 4, and 42 of 51 clones in mouse 5 had identical CDR3 sequences (Fig. 5*C*). However, these dominant VB5-2 clonotypes were different among the brains of mice. Similarly, dominant clonotypes obtained from VB8-2 had different CDR3 sequences among individual mice (Fig. 5*D*). These results indicated that oligoclonal T cells expanded in the brains of mice in response to WNV infection, and that the brain-infiltrating T cells used a highly restricted and shared TCRAV repertoire, but a somewhat diverse TCRBV repertoire.

To clarify T cell clonalities at an early time point during infection, we performed CDR3 sequence analyses using samples obtained from the brains on days 4 and 7 (Fig. 4). Brain T cells showed a more diverse TCR repertoire on days 4 and 7 compared with those on day 10 (Fig. 4*B*). On day 7, T cells showed some

degree of oligclonality, and interestingly, several clonotypes (CAVS-MG-NSGTYQRFG, CAVS-KG-NSGTYQRFG, and CAVS-IG-NSGTYQRFG) that presented dominantly on day 10 were obtained at low frequency on day 7 (Fig. 4*B*). These results suggest that oligoclonal T cells are generated by local expansion within the brains, not migration from the periphery.

Comparison of the TCR repertoire among closely related flaviviruses

TCR repertoires were also analyzed with spleens and brains from mice infected with closely related flaviviruses, JEV and TBEV (Fig. 6). The percentage frequencies of T cells bearing VA1-1, VA3-1, and VB9-1 were significantly higher in the brains of TBEV-infected mice than in the spleens from mock-infected mice. We have previously reported that the percentage frequencies of T cells bearing VA5-1, VA17-1, VA19-1, VB2-1, VB8-3, and VB13-1 were significantly increased in the brains of JEV-infected mice (7). These results demonstrated that TCR repertoires used by the brain-infiltrating T lymphocytes were different among WNV-,

A

	TCRAV repertoire	TCRBV repertoire

Column headers (TCRAV): 1-1, 1-2, 1-3, 2-1, 2-2, 3-1, 3-2, 4-1, 4-2, 4-3, 4-4, 4-5, 5-1, 6-1, 7-1, 8-1, 9-1, 10-1, 11-1, 12-1, 13-1, 14-1, 15-1, 16-1, 17-1, 18-1, 18-2, 19-1, 20-1

Column headers (TCRBV): 1-1, 2-1, 3-1, 4-1, 5-1, 5-2, 6-1, 7-1, 8-1, 8-2, 8-3, 9-1, 10-1, 11-1, 12-1, 13-1, 14-1, 15-1, 16-1, 17-1, 18-1, 19-1, 20-1

Rows: WNV, JEV, TBEV (filled boxes indicate repertoires increased in the brains, $p < 0.05$)

■ $P < 0.05$

B

VA1-1

Mock (Spleen) / TBEV (Spleen) / TBEV (Brain)

#1, #2, #3, #4, #5

160 170 180 190 Size (bp)

C

Brain	Clonal frequency	V	N	J	J gene	
#1	11/52	CAAS	ERG	YGGSGNKLIFG	AJ32	§
	8/52	CAAS	ERD	YGGSGNKLIFG	AJ32	¶
	6/52	CA	V	DSGYNKLTFG	AJ11	
	6/52	CA	VD	NTNTGKLTFGDG	AJ27	
	5/52	CAAS	ERY	YGGSGNKLIFG	AJ32	θ
	5/52	CAAS	ERF	YGGSGNKLIFG	AJ32	†
	2/52	CAAS	ERS	YGGSGNKLIFG	AJ32	‡
	1/52	CA	VF	MGYKLTFG	AJ09	
	1/52	CA	VSM	MGYKLTFG	AJ09	
	1/52	CAAS	VH	NNRIFFG	AJ31	
	1/52	CAAS	ERT	YGGSGNKLIFG	AJ32	ж
	1/52	CAAS	ERR	YGGSGNKLIFG	AJ32	
	1/52	CA	VSG	GGSGNKLIFG	AJ32	
	1/52	CA	V	SNYQLIWGSG	AJ33	
	1/52	CAA	F	NTGNYKYVFG	AJ40	
	1/52	CA	G	NNNNAPRFG	AJ43	
#2	14/51	CAAS	ERG	YGGSGNKLIFG	AJ32	§
	9/51	CAAS	ERN	YGGSGNKLIFG	AJ32	@
	6/51	CAA		DTNAYKVIFG	AJ30	
	4/51	CAAS	ERI	YGGSGNKLIFG	AJ32	й
	4/51	CAAS	ERE	YGGSGNKLIFG	AJ32	
	3/51	CAAS	ERY	YGGSGNKLIFG	AJ32	θ
	2/51	CAAS	ERD	YGGSGNKLIFG	AJ32	¶
	2/51	CAAS	ERA	YGGSGNKLIFG	AJ32	
	2/51	CAAS	ERP	YGGSGNKLIFG	AJ32	
	1/51	CAA	RG	QGGRALIFG	AJ15	
	1/51	CAAS	DP	NAYKVIFG	AJ30	
	1/51	CAAS	ERT	YGGSGNKLIFG	AJ32	ж
	1/51	CAA	REG	SSNTNKVVFG	AJ34	
	1/51	CA	V	NNNNAPRFG	AJ43	
#3	30/50	CAAS	IGD	MGYKLTFG	AJ09	
	5/50	CAAS	ERG	YGGSGNKLIFG	AJ32	§
	3/50	CAAS	EQN	YGGSGNKLIFG	AJ32	
	3/50	CAAS	ERN	YGGSGNKLIFG	AJ32	@
	2/50	CAAS	ERV	YGGSGNKLIFG	AJ32	
	2/50	CAAS	ERD	YGGSGNKLIFG	AJ32	¶
	1/50	CAAS	EQV	YGGSGNKLIFG	AJ32	
	1/50	CAAS	ERGW	GGSGNKLIFG	AJ32	
	1/50	CAA	H	YGSSGNKLIFG	AJ32	
	1/50	CAAS	GA	NTNKVVFG	AJ34	
	1/50	CA	ES	NNNNAPRFG	AJ43	

Brain	Clonal frequency	V	N	J	J gene	
#4	12/53	CAAS	ERN	YGGSGNKLIFG	AJ32	@
	9/53	CAAS	ERS	YGGSGNKLIFG	AJ32	‡
	6/53	CAAS	ERG	YGGSGNKLIFG	AJ32	§
	6/53	CAAS	G	GGRALIFG	AJ15	
	5/53	CAAS	ERI	YGGSGNKLIFG	AJ32	й
	2/53	CAAS	P	GGRALIFG	AJ15	
	2/53	CAA	IP	NYNVLYFG	AJ21	
	2/53	CAAS	W	NRIFFG	AJ31	
	1/53	CA	PP	NSAGNKLTFG	AJ17	
	1/53	CA	RT	NSAGNKLTFG	AJ17	
	1/53	CAAS	EGHT	ASLGKLQFG	AJ24	
	1/53	CA	V	DTNAYKVIFG	AJ30	д
	1/53	CAAS	ERSH	GGSGNKLIFG	AJ32	
	1/53	CAAS		NTGNYKYVFG	AJ40	
	1/53	CAAS	LDTG	GADRLTFG	AJ45	
	1/53	CAAS	EHD	YGNEKITFG	AJ48	
	1/53	CAAS	EGG	NYGNEKITFG	AJ48	
#5	11/52	CAAS	ERG	YGSSGNKLIFG	AJ32	§
	8/52	CA	G	NNAGAKLTFG	AJ39	
	7/52	CAAS	ERN	YGSSGNKLIFG	AJ32	@
	6/52	CAAS	E	GFASALTFG	AJ35	
	5/52	CA	V	DTNAYKVIFG	AJ30	д
	5/52	CAAS	EQR	YGSSGNKLIFG	AJ32	
	3/52	CA	V	NYAQG	AJ26	
	2/52	CAAS	ERF	YGGSGNKLIFG	AJ32	†
	1/52	CAAS	KA	GGYKVVFG	AJ12	
	1/52	CA	V	TGGYKVVFG	AJ12	
	1/52	CA	VMP	NYNVLYFG	AJ21	
	1/52	CAAS	N	GFASALTFG	AJ35	
	1/52	CA	VS	TGNTGKLIFG	AJ37	

FIGURE 6. Comparison of TCR repertoires of brain-infiltrating T lymphocytes among WNV-, JEV-, and TBEV-infected mice. A, TCRAV and TCRBV repertoires, which were increased in the brains by infection with WNV, JEV, or TBEV, are indicated by filled boxes ($p < 0.05$, Student unpaired t test, $n = 5$). TCR repertoire of T cells in JEV-infected mouse brains was reported previously (7). B, CDR3 size spectratyping of T cells bearing VA1-1 in TBEV-infected mouse brains. C, Amino acid sequences of CDR3 regions of VA1-1 in TBEV-infected mouse brains. Identical sequences detected in different individual mice are marked by the symbols.

TBEV-, and JEV-infected mice, with the exception of VA1-1, which increased significantly in WNV as well as TBEV (Fig. 6A). T cell clonality was examined in TBEV-infected mice brain, with a VA1-1–specifc primer by CDR3 size spectratyping (Fig. 6B). Oligoclonal peak patterns of T cells were detected in all five TBEV-infected mice. A dominant peak was identical in length among five mice. However, the length of the dominant peak was different between WNV- and TBEV-infected mice brain (Figs. 3B, 6B).

To examine whether these expanding T cells shared identical or similar TCR repertoires between WNV- and TBEV-infected mice, the nucleotide sequences of CDR3 were determined for VA1-1 cDNA clones from TBEV-infected mice (Fig. 6C). Nine clonotypes (CAAS-ERX-YGGSGNKLIFG; X of N region including G, D, Y, F, S, T, N, and I; and CA-V-DTNAYKVIFG) were detected in different mice. These clonotypes had highly similar CDR3 sequences and differed in a single amino acid residue within the N region. Additionally, preferential usage of AJ32 was observed in VA1-1 of the TBEV-infected brains. However, there was no similarity in CDR3 sequences between clonotypes obtained from WNV-infected and TBEV-infected mice. These results indicated that the brain-infiltrating T cells induced by closely related viruses, namely WNV, JEV, and TBEV, did not use shared TCR repertoires.

Cross-reaction of brain-infiltrating T cells between WNV and JEV in vitro

The specificity and cross-reactivity of brain-infiltrating T cells were examined. T cells isolated from either WNV- or JEV-infected C3H/HeN (H-2k) mouse brains were cultured for 12 h with PECs infected with WNV or JEV. Levels of IFN-γ and TNF-α were assessed by ELISA in the culture supernatant fluids (Table II). High levels of IFN-γ and TNF-α were detected in the supernatants of T cells from WNV-infected mouse brains after stimulation with WNV-infected PECs of C3H/HeN mice, but not after stimulation with JEV-infected PECs of C3H/HeN mice or WNV-infected PECs from mice with different MHC haplotypes. High IFN-γ and TNF-α production was also detected in the supernatants of T cells from JEV-infected mouse brains only after stimulation with JEV-infected PECs of C3H/HeN mice. Additionally, in vitro stimulation of CD4⁺ or CD8⁺ cells isolated separately from WNV-infected mouse brain was performed (Table III). The results

Table II. IFN-γ and TNF-α production by T cells isolated from WNV- or JEV-infected C3H/HeN mouse brains after in vitro stimulation with WNV or JEV

PECs Isolated from	Virus Infection	IFN-γ Production (pg/ml)		TNF-α Production (pg/ml)	
		T Cells Isolated from WNV-Infected C3H/HeN Mice Brain	T Cells Isolated from JEV-Infected C3H/HeN Mice Brain	T Cells Isolated from WNV-Infected C3H/HeN Mice Brain	T Cells Isolated from JEV-Infected C3H/HeN Mice Brain
C3H/HeNJcl (H-2^k)	WNV	1446.6 ± 55.5	20.3 ± 8.5	476.9 ± 46.7	26.4 ± 9.8
	JEV	18.7 ± 3.1	1038.2 ± 53.4	19.8 ± 7.2	370.1 ± 84.1
	None	18.3 ± 4.5	17.5 ± 6.5	22.7 ± 3.1	25.2 ± 4.9
C57BL/6JJcl (H-2^b)	WNV	24.1 ± 7.2	22.1 ± 4.4	21.9 ± 6.1	25.3 ± 7.4
	JEV	26.3 ± 8.6	24.7 ± 3.9	19.2 ± 4.3	24.2 ± 5.4
	None	25.0 ± 6.5	20.1 ± 4.2	23.3 ± 5.9	26.2 ± 6.2
BALB/cAJcl (H-2^d)	WNV	15.7 ± 2.5	21.1 ± 7.1	27.2 ± 8.4	24.1 ± 4.7
	JEV	18.9 ± 3.6	23.7 ± 5.8	26.3 ± 6.0	24.4 ± 1.2
	None	23.3 ± 7.5	24.7 ± 2.2	27.0 ± 9.1	29.6 ± 3.3

Levels of IFN-γ and TNF-α were assessed by ELISA in the supernatants of T cells isolated from WNV- or JEV-infected mouse brains (n = 8) after in vitro stimulation for 12 h with PECs infected with WNV or JEV. Numbers indicate the mean ± SD of IFN-γ and TNF-α production (pg/ml) in triplicate wells.

indicate that CD8$^+$ cells isolated from the brains of mice infected with WNV were virus-specific, but not cross-reactive, between WNV and JEV, and that CD4$^+$ T cells were not WNV-specific.

T cells from WNV-infected mouse brains were cultured with PECs infected with WNV for 3 d. CDR3 sequences of VA1-1 and VA2-1 were compared before and after in vitro stimulation (Table IV). Before stimulation, the pooled T cells exhibited oligoclonality with several TCR clonotypes that were identical to the dominant TCR clonotypes found in five individual mice in Fig. 5. After stimulation for 3 d, the T cells also showed extensive clonality for both VA1-1 and VA2-1 (Table IV). The dominant CDR3 sequences were maintained after stimulation, suggesting the expansion of specific T cell clones.

Discussion

WNV (strain NY99-6922) induced encephalitis in C3H/HeN mice after i.p. administration. Histopathological analysis demonstrated encephalitic changes, CNS degeneration, and infiltration of CD3$^+$ CD8$^+$ T cells in the brains of WNV-infected mice. This corresponds to the fact that the expression level of CD3 and CD8 positively correlated with viral RNA levels in the brains of WNV-infected mice. These results suggest that CD8$^+$ T cells predominantly infiltrated in the brains as infection progressed. It has been reported that tissue destruction and the presence of CD3$^+$ CD8$^+$ T cells were found in the brains of JEV- and TBEV-infected mice (7, 24). There are reports on human T cell responses following in vitro stimulation of PBMCs from WNV-infected patients with peptides derived from WNV Ags (25, 26). They indicated a critical role of CD8$^+$ T cells and IFN-γ production in responses to a limited number of epitopes with MHC restriction. The similar nature of T cell immunity between humans and mice

supports the idea that the murine model in the present study is useful for elucidating the characteristics of brain-infiltrating T cells during flavivirus infection. This will lead to greater understanding of T cell immune responses in WNV-infected humans.

CD4$^+$ cells were stained and their transcripts were persistently expressed at a high level in both mock and infected mouse brains. This is probably due to the presence of microglia that express CD4 in CNS resident cells (27, 28). These results do not necessarily mean that CD4$^+$ T cells are absent in the WNV-infected brains. It has been reported that both CD4$^+$ and CD8$^+$ T cells increase in the brains after WNV infection (29). The CD4 transcripts expressed by the microglia, which are abundantly present in the CNS, might mask more CD4$^+$ T cells in the brains. Notably, the expression level of the contents of cytotoxic granules, such as perforin, granzyme A, and granzyme B, were positively related to the increase in CD8 in the brain. These cytotoxicity-related genes were mainly expressed in activated CD8$^+$ cells or NK cells, but not in CD4$^+$ cells. It is known that CD8$^+$ T cells are activated separately from NK cells in WNV-infected mouse brains (30). These results suggest that most of the brain-infiltrating T lymphocytes are cytotoxic CD8$^+$ T cells.

Th1-type cytokines were largely induced in the brains in response to WNV infection. The increased expression of IFN-γ, TNF-α, and IL-2 were remarkable on day 10 after viral infection, suggesting that Th1 cytokine-producing T cells contribute to antiviral response in the CNS. It is of interest that IL-10 was abundantly expressed in both the spleens and brains. A recent report demonstrated that IL-10 was mainly produced by CD4$^+$ cells and was dramatically elevated in WNV-infected mice (31). Given that IL-10 controls host immune responses by suppressing Th1 responses (32), elevated production of IL-10 impacts on WNV

Table III. IFN-γ and TNF-α production by CD8$^+$ cells, but not CD4$^+$ cells, isolated from WNV-infected C3H/HeN mouse brains after in vitro stimulation with WNV- or JEV-infected PECs in C3H/HeN mice

C3H/HeN PECs Infected with	Isolated Cells from WNV-Infected C3H/HeN Mice Brain			
	IFN-γ Production (pg/ml)		TNF-α Production (pg/ml)	
	CD4$^+$ Cells	CD8$^+$ Cells	CD4$^+$ Cells	CD8$^+$ Cells
WNV	15.4 ± 4.2	1358.1 ± 74.5	26.4 ± 3.9	623.6 ± 49.2
JEV	17.1 ± 4.7	19.8 ± 8.2	23.9 ± 5.8	23.1 ± 6.1
None	16.6 ± 6.1	24.7 ± 6.9	24.1 ± 7.7	28.5 ± 2.7

Levels of IFN-γ and TNF-α were assessed by ELISA in supernatants of CD4$^+$ or CD8$^+$ cells isolated from WNV-infected mouse brains (n = 8) after in vitro stimulation for 12 h with PECs infected with WNV or JEV. Numbers indicate the mean ± SD of IFN-γ and TNF-α production (pg/ml) in three wells.

Table IV. T cell clonalities in WNV-infected mouse brains before and after in vitro stimulation with PECs infected with WNV

Clonal Frequency	V	N	J	J Gene[a]	Frequency[b]
VA1-1 (prestimulation)					
12/55	CAVS	IG	NSGTYQRFG	AJ13 #	2/5
10/55	CAVS	LA	NSGTYQRFG	AJ13 $	1/5
8/55	CAVS	MG	NSGTYQRFG	AJ13 §	3/5
7/55	CAVS	KG	NSGTYQRFG	AJ13 †	2/5
6/55	CAV	RPT	ASLGKLQFG	AJ24 ‡	1/5
4/55	CAVS	PG	NSGTYQRFG	AJ13	2/5
4/55	CAVS		TNAYKVIFG	AJ30	0/5
2/55	CAVS	RG	NSGTYQRFG	AJ13	1/5
1/55	CAVS	RG	QGGRALIFG	AJ15	1/5
1/55	CAVS	MG	GYQNFYFG	AJ49	2/5
VA1-1 (poststimulation)[d]					
37/52	CAVS	IG	NSGTYQRFG	AJ13 #	2/5
10/52	CAVS	MG	NSGTYQRFG	AJ13 §	3/5
3/52	CAVS	KG	NSGTYQRFG	AJ13 †	2/5
1/52	CAVS	LA	NSGTYQRFG	AJ13 $	1/5
1/52	CAV	RPT	ASLGKLQFG	AJ24 ‡	1/5
VA2-1 (prestimulation)[c]					
14/51	CAAS	EA	GNYKYVFG	AJ40 #	4/5
11/51	CAAS	EG	GNYKYVFG	AJ40 $	2/5
7/51	CAAS	G	GSALGRLHFG	AJ18	1/5
6/51	CAA	RG	NNYAQGLTFG	AJ26 §	1/5
4/51	CAAS	VA	GNYKYVFG	AJ40 †	1/5
3/51	CAAS	G	NNYAQGLTFG	AJ26	1/5
2/51	CAAS	NA	NAYKVIFG	AJ30	1/5
2/51	CAA	I	TGGNNKLTFG	AJ56	1/5
1/51	CA	PRG	NNYAQGLTFG	AJ26	1/5
1/51	CAAS	P	TNAYKVIFG	AJ30	1/5
VA2-1 (poststimulation)[d]					
35/54	CAAS	EG	GNYKYVFG	AJ40 $	2/5
16/54	CAAS	EA	GNYKYVFG	AJ40 #	4/5
2/54	CAA	RG	NNYAQGLTFG	AJ26 §	1/5
1/54	CAAS	VA	GNYKYVFG	AJ40 †	1/5

[a]Identical sequences observed in both pre- and poststimulation are marked by respective symbols in the column.
[b]The frequency indicates the number of mice, among a total of five, where the clones with the respective CDR3 sequences were detected in Fig. 5.
[c]T cells were isolated from eight WNV-infected C3H/HeN mouse brains and pooled ($n = 8$). CDR3 regions of cDNA clones containing VA1-1 and VA2-1 were sequenced.
[d]T cells were stimulated in vitro with PECs infected with WNV at 37°C for 3 d and were subjected to CDR3 sequence analysis.

pathogenesis by preventing the host from inducing a hyper-inflammatory immune reaction. It is known that chemokines and chemokine receptors are important to the pathogenesis of WNV infection. Microglia and astrocytes secrete the chemokines CCL5 and CXCL10 (33), which recruit effector T cells via the chemokine receptors CXCR3 (19, 34) and CCR5 (29) in C57BL/6J mice, respectively. The expression levels of the chemokines CCL5 and CXCL10 increased >100-fold in the brains, whereas the increases in their receptors, CCR5 and CXCR3, were not as pronounced in C3H mice. As has been previously reported (35), the expression levels of early (CD25) and late (CD69) T cell activation markers were increased with time. Thus, it is likely that the brain-infiltrating T lymphocytes are mostly supplied by local expansion of CD8^{+} T cells, rather than by the recruitment of CCR5^{+} or CXCR3^{+} T cells across the blood–brain barrier by the CCL5 and CXCL10.

TCR mRNA was below detectable levels in the mock brains because of poor infiltration of T cells. In contrast, TCR expression was ~100-fold higher in WNV-infected brains on day 10 compared with mock-infected brains. There is a possibility that the accumulation of T cells in the brains is caused by nonspecific migration from peripheral organs and random leakage from pe-

ripheral blood. However, the T cells showed high oligoclonality in their TCR repertoires that were completely different between WNV-infected mice and JEV-infected mice. Moreover, a few T cells that resided within the brains increased drastically from day 7 to day 10. These results suggest that the increase in the number of CD8^{+} T cells in the brains is mainly due to local expansion of T cells that recognize different Ags among closely related viruses.

TCR usage was found to be completely different between WNV- and JEV-infected mice brains; this is not, however, consistent with cross-reactivity of Abs between WNV and JEV (15). MHC-restricted cytotoxic T cells against WNV-infected target cells were detected in mice (36, 37), and mouse spleen cells immunized with JEV partially lysed WNV-infected target cells (38, 39). Peptide variants derived from 9-aa residues of NS4b elicit cross-reactive CD8^{+} T cells in both JEV and WNV, whereas their functional and phenotypic properties were different between JEV and WNV (40). In our studies, the brain-infiltrating CD8^{+} T cells showed a similar characteristic, namely a Th1/Tc1 phenotype, between WNV- and JEV-infected mice. CD8^{+} T cells isolated from virus-infected mouse brains produced IFN-γ and TNF-α after coculture in vitro with virus-infected PECs with syngeneic

MHC haplotype, suggesting that the $CD8^+$ T cells within brains are virus-specific and not cross-reactive with other flaviviruses. Moreover, dominant T cells with a high clonality were detected in the brains of different individual mice, suggesting that they were not induced by bystander activation of nonspecific T cells. These results strongly suggest that the dominant T cells elicited in brains by in vivo primary WNV infection are virus-specific and not crossreactive. It is possible that the cross-reactive T cells are subdominant in the brain following primary WNV infection. Cellular cloning techniques or sequential stimulation in vitro with Ag probably induce a skewed hierarchy of T cells and may not be genuinely representative of the in vivo T cell populations. The direct cloning of TCR genes from local inflammatory sites would be a powerful tool for understanding T cell-mediated immunopathology and recovery in WNV encephalitis.

CDR3 sequence analysis revealed interesting results on Ag specificity. Most TCR clonotypes obtained from the brains of flavivirus-infected mice showed preferential usage of AJ segments (AJ13 for VA1-1 of WNV, AJ40 for VA2-1 of WNV, AJ32 for VA1-1 of TBEV). For WNV-infected mice, TCR clonotypes derived from VA1-1 contained rich hydrophobic amino acids such as alanine, glycine, isoleucine, leucine, methionine, and proline in the N region (126 of 154 residues). TBEV-infected mice frequently used an ERX motif (for glutamate, arginine, and X, which represents any amino acid), which contains polar amino acids in the N region. The dissimilarity in CDR3α sequences suggests the expansion of T cells with different Ag specificities between WNV-infected mice and TBEV-infected mice. The brain-infiltrating T lymphocytes did not share identical TCR repertoires between WNV-infected and JEV-infected mice (7).

In contrast to the very restricted TCRAV repertoire, the brain-infiltrating T lymphocytes exhibited relatively broad TCRBV repertoires. In VB5-2, CDR3 sequences varied considerably among individual mice, although BJ usage was limited to BJ2.1 and BJ2.7. Similarly, a common CDR3 sequence was not found in VB8-2 among individual mice. This contrasting result probably reflects a different role of TCR α- and β-chains in Ag recognition. The difference in the extent of repertoire restriction between TCR α- and β-chains has been shown in mice infected with JEV, a closely related flavivirus (7). Usage of restricted TCRAV and broad TCRBV has been reported in infection with other viruses, such as herpesvirus (41). Moreover, several reports have also described a dominant and essential role of the TCR α-chain in Ag recognition by T cells (42–44). It has been reported that TCRαβ heterodimers bearing a restricted TCR α-chain and diverse TCR β-chains have the potential to specifically recognize a single Ag in vitro (45). The dominant role of TCR α-chain is reflected to the restriction of the TCR β-chain repertoire observed in the brain-infiltrating T lymphocytes of WNV-infected mice.

We defined day 10 as the humane endpoint because this WNV-infected encephalitis mouse model was produced by administration of a lethal dose of the virus. Therefore, we could not observe $CD8^+$ T cell immune responses at later time points in animals that had recovered or not. It is known that the mortality rate is higher in CD8KO mice than in control mice and that $CD8^+$ T cells within the brain could play a protective role in the hosts (5). We recently reported that T cells that migrated into the brain following administration of a low dose of TBEV were different between living and dying mice (46). Further studies are needed to clarify the protective or immunopathological role of $CD8^+$ T cells by using low-dose administration of WNV.

In conclusion, Th1-like cytotoxic $CD8^+$ T cells with high clonality infiltrate into the brains of WNV-infected mice. These oligoclonal brain-infiltrating T cells use unique TCR repertoires, which

are generated by a limited TCRα and diverse TCRβ genes. Moreover, the dominant brain-infiltrating $CD8^+$ T cells elicited in vivo by primary WNV infection are virus-specific, but not cross-reactive, among related flaviviruses. The present study provides important information on Ag specificity and diversity of WNV-specific $CD8^+$ T cells, as well as a new insight into the critical role of brain-infiltrating T cells in the recovery from WNV infection.

Acknowledgments

Disclosures

The authors have no financial conflicts of interest.

References

1. Petersen, L. R., and A. A. Marfin. 2002. West Nile virus: a primer for the clinician. *Ann. Intern. Med.* 137: 173–179.
2. Petersen, L. R., and J. T. Roehrig. 2001. West Nile virus: a reemerging global pathogen. *Emerg. Infect. Dis.* 7: 611–614.
3. Watson, J. T., P. E. Pertel, R. C. Jones, A. M. Siston, W. S. Paul, C. C. Austin, and S. I. Gerber. 2004. Clinical characteristics and functional outcomes of West Nile fever. *Ann. Intern. Med.* 141: 360–365.
4. Dauphin, G., S. Zientara, H. Zeller, and B. Murgue. 2004. West Nile: worldwide current situation in animals and humans. *Comp. Immunol. Microbiol. Infect. Dis.* 27: 343–355.
5. Shrestha, B., and M. S. Diamond. 2004. Role of $CD8^+$ T cells in control of West Nile virus infection. *J. Virol.* 78: 8312–8321.
6. Purtha, W. E., N. Myers, V. Mitaksov, E. Sitati, J. Connolly, D. H. Fremont, T. H. Hansen, and M. S. Diamond. 2007. Antigen-specific cytotoxic T lymphocytes protect against lethal West Nile virus encephalitis. *Eur. J. Immunol.* 37: 1845–1854.
7. Fujii, Y., K. Kitaura, K. Nakamichi, T. Takasaki, R. Suzuki, and I. Kurane. 2008. Accumulation of T-cells with selected T-cell receptors in the brains of Japanese encephalitis virus-infected mice. *Jpn. J. Infect. Dis.* 61: 40–48.
8. Davis, M. M. 1990. T cell receptor gene diversity and selection. *Annu. Rev. Biochem.* 59: 475–496.
9. Ding, Y. H., K. J. Smith, D. N. Garboczi, U. Utz, W. E. Biddison, and D. C. Wiley. 1998. Two human T cell receptors bind in a similar diagonal mode to the HLA-A2/Tax peptide complex using different TCR amino acids. *Immunity* 8: 403–411.
10. Gotoh, A., Y. Hamada, N. Shiobara, K. Kumagai, K. Seto, T. Horikawa, and R. Suzuki. 2008. Skew in T cell receptor usage with polyclonal expansion in lesions of oral lichen planus without hepatitis C virus infection. *Clin. Exp. Immunol.* 154: 192–201.
11. Matsutani, T., K. Shiiba, T. Yoshioka, Y. Tsuruta, R. Suzuki, T. Ochi, T. Itoh, H. Musha, T. Mizoi, and I. Sasaki. 2004. Evidence for existence of oligoclonal tumor-infiltrating lymphocytes and predominant production of T helper 1/T cytotoxic 1 type cytokines in gastric and colorectal tumors. *Int. J. Oncol.* 25: 133–141.
12. Shiobara, N., Y. Suzuki, H. Aoki, A. Gotoh, Y. Fujii, Y. Hamada, S. Suzuki, N. Fukui, I. Kurane, T. Itoh, and R. Suzuki. 2007. Bacterial superantigens and T cell receptor β-chain-bearing T cells in the immunopathogenesis of ulcerative colitis. *Clin. Exp. Immunol.* 150: 13–21.
13. Kitaura, K., K. Kanayama, Y. Fujii, N. Shiobara, K. Tanaka, I. Kurane, S. Suzuki, T. Itoh, and R. Suzuki. 2009. T cell receptor repertoire in BALB/c mice varies according to tissue type, sex, age, and hydrocortisone treatment. *Exp. Anim.* 58: 159–168.
14. Matsutani, T., T. Ohmori, M. Ogata, H. Soga, T. Yoshioka, R. Suzuki, and T. Itoh. 2006. Alteration of T-cell receptor repertoires during thymic T-cell development. *Scand. J. Immunol.* 64: 53–60.
15. Lim, C. K., T. Takasaki, A. Kotaki, and I. Kurane. 2008. Vero cell-derived inactivated West Nile (WN) vaccine induces protective immunity against lethal WN virus infection in mice and shows a facilitated neutralizing antibody response in mice previously immunized with Japanese encephalitis vaccine. *Virology* 374: 60–70.
16. Takashima, I., K. Morita, M. Chiba, D. Hayasaka, T. Sato, C. Takezawa, A. Igarashi, H. Kariwa, K. Yoshimatsu, J. Arikawa, and N. Hashimoto. 1997. A case of tick-borne encephalitis in Japan and isolation of the the virus. *J. Clin. Microbiol.* 35: 1943–1947.
17. Hayasaka, D., L. Ivanov, G. N. Leonova, A. Goto, K. Yoshii, T. Mizutani, H. Kariwa, and I. Takashima. 2001. Distribution and characterization of tick-borne encephalitis viruses from Siberia and far-eastern Asia. *J. Gen. Virol.* 82: 1319–1328.
18. Kasahara, T., T. Miyazaki, H. Nitta, A. Ono, T. Miyagishima, T. Nagao, and T. Urushidani. 2006. Evaluation of methods for duration of preservation of RNA quality in rat liver used for transcriptome analysis. *J. Toxicol. Sci.* 31: 509–519.

19. Klein, R. S., E. Lin, B. Zhang, A. D. Luster, J. Tollett, M. A. Samuel, M. Engle, and M. S. Diamond. 2005. Neuronal CXCL10 directs CD8+ T-cell recruitment and control of West Nile virus encephalitis. *J. Virol.* 79: 11457–11466.

20. Matsutani, T., T. Yoshioka, Y. Tsuruta, S. Iwagami, and R. Suzuki. 1997. Analysis of TCRAV and TCRBV repertoires in healthy individuals by microplate hybridization assay. *Hum. Immunol.* 56: 57–69.

21. Tsuruta, Y., S. Iwagami, S. Furue, H. Teraoka, T. Yoshida, T. Sakata, and R. Suzuki. 1993. Detection of human T cell receptor cDNAs (α, β, γ and δ) by ligation of a universal adaptor to variable region. *J. Immunol. Methods* 161: 7–21.

22. Yoshida, R., T. Yoshioka, S. Yamane, T. Matsutani, T. Toyosaki-Maeda, Y. Tsuruta, and R. Suzuki. 2000. A new method for quantitative analysis of the mouse T-cell receptor V region repertoires: comparison of repertoires among strains. *Immunogenetics* 52: 35–45.

23. Horiuchi, T., M. Hirokawa, Y. Kawabata, A. Kitabayashi, T. Matsutani, T. Yoshioka, Y. Tsuruta, R. Suzuki, and A. B. Miura. 2001. Identification of the T cell clones expanding within both CD8+CD28+ and CD8+CD28− T cell subsets in recipients of allogeneic hematopoietic cell grafts and its implication in post-transplant skewing of T cell receptor repertoire. *Bone Marrow Transplant.* 27: 731–739.

24. Hayasaka, D., N. Nagata, Y. Fujii, H. Hasegawa, T. Sata, R. Suzuki, E. A. Gould, I. Takashima, and S. Koike. 2009. Mortality following peripheral infection with tick-borne encephalitis virus results from a combination of central nervous system pathology, systemic inflammatory and stress responses. *Virology* 390: 139–150.

25. Lanteri, M. C., J. W. Heitman, R. E. Owen, T. Busch, N. Gefter, N. Kiely, H. T. Kamel, L. H. Tobler, M. P. Busch, and P. J. Norris. 2008. Comprehensive analysis of West Nile virus-specific T cell responses in humans. *J. Infect. Dis.* 197: 1296–1306.

26. Parsons, R., A. Lelic, L. Hayes, A. Carter, L. Marshall, C. Evelegh, M. Drebot, M. Andonova, C. McMurtrey, W. Hildebrand, et al. 2008. The memory T cell response to West Nile virus in symptomatic humans following natural infection is not influenced by age and is dominated by a restricted set of CD8+ T cell epitopes. *J. Immunol.* 181: 1563–1572.

27. Omri, B., P. Crisanti, F. Alliot, M. C. Marty, J. Rutin, C. Levallois, A. Privat, and B. Pessac. 1994. CD4 expression in neurons of the central nervous system. *Int. Immunol.* 6: 377–385.

28. Alliot, F., M. C. Marty, D. Cambier, and B. Pessac. 1996. A spontaneously immortalized mouse microglial cell line expressing CD4. *Brain Res. Dev. Brain Res.* 95: 140–143.

29. Glass, W. G., J. K. Lim, R. Cholera, A. G. Pletnev, J. L. Gao, and P. M. Murphy. 2005. Chemokine receptor CCR5 promotes leukocyte trafficking to the brain and survival in West Nile virus infection. *J. Exp. Med.* 202: 1087–1098.

30. Liu, Y., R. V. Blanden, and A. Müllbacher. 1989. Identification of cytolytic lymphocytes in West Nile virus-infected murine central nervous system. *J. Gen. Virol.* 70: 565–573.

31. Bai, F., T. Town, F. Qian, P. Wang, M. Kamanaka, T. M. Connolly, D. Gate, R. R. Montgomery, R. A. Flavell, and E. Fikrig. 2009. IL-10 signaling blockade controls murine West Nile virus infection. *PLoS Pathog.* 5: e1000610.

32. Moore, K. W., R. de Waal Malefyt, R. L. Coffman, and A. O'Garra. 2001. Interleukin-10 and the interleukin-10 receptor. *Annu. Rev. Immunol.* 19: 683–765.

33. Cheeran, M. C., S. Hu, W. S. Sheng, A. Rashid, P. K. Peterson, and J. R. Lokensgard. 2005. Differential responses of human brain cells to West Nile virus infection. *J. Neurovirol.* 11: 512–524.

34. Zhang, B., Y. K. Chan, B. Lu, M. S. Diamond, and R. S. Klein. 2008. CXCR3 mediates region-specific antiviral T cell trafficking within the central nervous system during West Nile virus encephalitis. *J. Immunol.* 180: 2641–2649.

35. Wang, Y., M. Lobigs, E. Lee, and A. Müllbacher. 2003. CD8+ T cells mediate recovery and immunopathology in West Nile virus encephalitis. *J. Virol.* 77: 13323–13334.

36. Kesson, A. M., R. V. Blanden, and A. Mullbacher. 1987. The primary in vivo murine cytotoxic T cell response to the flavivirus, West Nile. *J. Gen. Virol.* 68: 2001–2006.

37. Uren, M. F., P. C. Doherty, and J. E. Allan. 1987. Flavivirus-specific murine L3T4+ T cell clones: induction, characterization and cross-reactivity. *J. Gen. Virol.* 68: 2655–2663.

38. Hill, A. B., A. Müllbacher, C. Parrish, G. Coia, E. G. Westaway, and R. V. Blanden. 1992. Broad cross-reactivity with marked fine specificity in the cytotoxic T cell response to flaviviruses. *J. Gen. Virol.* 73: 1115–1123.

39. Murali-Krishna, K., V. Ravi, and R. Manjunath. 1994. Cytotoxic T lymphocytes raised against Japanese encephalitis virus: effector cell phenotype, target specificity and in vitro virus clearance. *J. Gen. Virol.* 75: 799–807.

40. Trobaugh, D. W., L. Yang, F. A. Ennis, and S. Green. 2010. Altered effector functions of virus-specific and virus cross-reactive CD8+ T cells in mice immunized with related flaviviruses. *Eur. J. Immunol.* 40: 1315–1327.

41. Dong, L., P. Li, T. Oenema, C. L. McClurkan, and D. M. Koelle. 2010. Public TCR use by herpes simplex virus-2-specific human CD8 CTLs. *J. Immunol.* 184: 3063–3071.

42. Dietrich, P. Y., F. A. Le Gal, V. Dutoit, M. J. Pittet, L. Trautman, A. Zippelius, I. Cognet, V. Widmer, P. R. Walker, O. Michielin, et al. 2003. Prevalent role of TCR α-chain in the selection of the preimmune repertoire specific for a human tumor-associated self-antigen. *J. Immunol.* 170: 5103–5109.

43. Messaoudi, I., J. LeMaoult, B. M. Metzner, M. J. Miley, D. H. Fremont, and J. Nikolich-Zugich. 2001. Functional evidence that conserved TCR CDRα3 loop docking governs the cross-recognition of closely related peptide:class I complexes. *J. Immunol.* 167: 836–843.

44. Trautmann, L., N. Labarrière, F. Jotereau, V. Karanikas, N. Gervois, T. Connerotte, P. Coulie, and M. Bonneville. 2002. Dominant TCR Vα usage by virus and tumor-reactive T cells with wide affinity ranges for their specific antigens. *Eur. J. Immunol.* 32: 3181–3190.

45. Yokosuka, T., K. Takase, M. Suzuki, Y. Nakagawa, S. Taki, H. Takahashi, T. Fujisawa, H. Arase, and T. Saito. 2002. Predominant role of T cell receptor (TCR)-α chain in forming preimmune TCR repertoire revealed by clonal TCR reconstitution system. *J. Exp. Med.* 195: 991–1001.

46. Fujii, Y., D. Hayasaka, K. Kitaura, T. Takasaki, R. Suzuki, and I. Kurane. 2011. T cell clones expressing different T cell receptors accumulate in the brains of dying and surviving mice following peripheral infection with tick-borne encephalitis virus. *Viral Immunol.* In press.

T-Cell Clones Expressing Different T-Cell Receptors Accumulate in the Brains of Dying and Surviving Mice After Peripheral Infection with Far Eastern Strain of Tick-Borne Encephalitis Virus

Yoshiki Fujii,[1,2] Daisuke Hayasaka,[3] Kazutaka Kitaura,[1,2]
Tomohiko Takasaki,[1] Ryuji Suzuki,[2] and Ichiro Kurane[1]

Abstract

Tick-borne encephalitis virus (TBEV), a representative acute central nervous system disease-inducible virus, is known to elicit dose-independent mortality in a mouse model. We previously reported that subcutaneous infection with a wide range of TBEV Oshima strain challenge doses (10^2–10^6 PFU) produced an approximately 50% mortality rate. However, the factors playing critical roles in mortality and severity remain unclear. In this study, we distinguished surviving and dying mice by their degree of weight loss after TBEV infection, and investigated qualitative differences in brain-infiltrating T cells between each group by analyzing T-cell receptor (TCR) repertoire and complementary determining region 3 (CDR3) sequences. TCR repertoire analysis revealed that the expression levels of VA8-1, VA15-1, and VB8-2 families were increased in brains derived from both surviving and dying mice. CDR3 amino acid sequence characteristics differed between each group. In dying mice, high frequencies of VA15-1/AJ12 and VB8-2/BJ1.1 gene usage were observed. While in surviving mice, high frequencies of VA8-1/AJ15 or VA8-1/AJ23 gene usage were observed. VB8-2/BJ2.7 gene usage and short CDR3 were observed frequently in both surviving and dying mice. However, no differences in T-cell activation markers and apoptosis-related genes were observed between these groups using quantitative real-time PCR analysis. These results suggest that TBEV-infection severity may be involved in antigen specificity, but not in the number or activation level of brain-infiltrating T cells.

Introduction

TICK-BORNE ENCEPHALITIS VIRUS (TBEV) is a positive-sense single-stranded RNA virus of the family Flaviviridae that also includes Japanese encephalitis virus (JEV), West Nile virus (WNV), St. Louis encephalitis virus, and Murray Valley encephalitis virus. TBEV is an important causative agent of acute central nervous system disease in humans (8, 27). TBEV is distributed widely throughout Europe and Asia, and is genetically divided into three closely-related subtypes: the European, Siberian, and Far Eastern subtypes (9,20). The Far Eastern subtype is also distributed in southern parts of Hokkaido, Japan (38–40).

Clinical manifestations caused by TBEV range from inapparent infections and fevers, with complete recovery of patients, to debilitating or fatal encephalitis. While such diverse manifestations can be caused by any of the three subtypes (16,17), the percentage of severe cases differs among each subtype. We previously reported that differences exist in the severity of symptoms among individual mice after peripheral infection with the Oshima strain of TBEV, a member of the Far Eastern subtype (6,18,21). Following subcutaneous infection with a wide range of challenge doses (10^2–10^6 PFU), the mortality rate was consistently approximately 50% (21). Although a dose-independent mortality pattern is shown in several encephalitic flavivirus infection models, the causative biological mechanisms have yet to be defined (24,26,35,42,44,45). Thus, we investigated the immunological and biological responses in surviving and dying mice, so that increased corticosteroid serum levels and TNF-α

[1]Department of Virology 1, National Institute of Infectious Diseases, Tokyo, Japan.
[2]Department of Rheumatology and Clinical Immunology, Clinical Research Center for Allergy and Rheumatology, Sagamihara National Hospital, National Hospital Organization, Sagamihara, Japan.
[3]Department of Virology, Institute of Tropical Medicine, Nagasaki University, Nagasaki, Japan.

expression levels in the serum and the brains were observed in dying mice (21). However, as there was no significant difference in viral loads and the levels of cellular infiltration in the brains between the two groups, the fate of infected mice was not likely to be determined by neuro-invasiveness or the number of brain-infiltrating cells.

Multiple complex factors are associated with encephalitis pathogenesis. Recent studies indicate that brain-infiltrating T cells play an important role in viral encephalitis (24,26,34,45). T cells potentially contribute to both recovery and immunopathogenesis, and the functional balance between these differs among virus species and experimental conditions. For example, it is widely thought that T-cell responses are essential for viral clearance in WNV infection (4,5,15,32,36,37), although differences in responses between surviving and dying mice under identical inoculation conditions have not been determined. We further reported no differences in the number of brain-infiltrating CD8$^+$ T cells in our previous study (21), but did not compare immunological markers.

We previously demonstrated that T cells with selected T-cell receptors (TCRs) accumulate in JEV-infected mouse brains using TCR repertoire analysis and nucleotide sequencing of the complementary determining region 3 (CDR3) (10). These are efficient methods for analyzing relative expression levels of each TCR family and the frequency of each T-cell clone, which allows us to better understand the pathological and/or protective mechanism in our TBEV-infected mouse model. By determining the TCR repertoire and frequencies of T-cell clones we can assess if different patterns exist between surviving and dying mice. Identical patterns would indicate that disease severity is independent of T cells, whereas different patterns would indicate that T-cell antigen recognition pattern is related to severity. The purpose of our study was therefore to clarify whether T cells influence the severity of TBEV-induced encephalitis.

Materials and Methods

Virus and cells

Stock virus of TBEV Oshima 5-10 strain (accession no. AB062063) was prepared from the medium used to culture baby hamster kidney (BHK) cells after five passages through suckling mouse brains (20). BHK cells were maintained in Eagle's Minimal Essential Medium (EMEM; Nissui Pharmaceutical Co., Tokyo, Japan) containing 8% fetal calf serum (FCS). All experiments using live TBEV were performed in a biosafety level three (BSL3) laboratory at the Tokyo Metropolitan Institute for Neuroscience according to the standard BSL3 guidelines.

Mice

Five-week old female C57BL/6j mice were subcutaneously inoculated with 10^3 PFU of TBEV diluted in EMEM containing 2% FCS. Mock-infected mice were inoculated with EMEM from the supernatant medium of BHK cells. Mice were weighed daily and observed for clinical disease symptoms including behavioral symptoms and signs of paralysis. Morbidity was determined as relative weight loss compared with day 0. Thirteen days post-infection (dpi), mice exhibiting more than 25% or less than 10% weight loss were recognized as dying or surviving mice, respectively

(21). The Animal Care and Use Committee of the Tokyo Metropolitan Institute for Neuroscience approved all experimental protocols.

Isolation of total RNA from tissues

Mice injected with mock or TBEV were anesthetized and perfused with cold PBS at 13 dpi. Brains and spleens were excised and immediately submerged in RNA*later*® RNA Stabilization Reagent (Qiagen, Hilden, Germany). Total RNA was then isolated using an RNeasy Lipid Tissue Mini kit (Qiagen) according to the manufacturer's instructions. Isolated total RNA was used for TCR repertoire analysis, CDR3 sequencing, and quantification of viral RNA and gene expressions using quantitative real-time PCR.

Adaptor ligation-mediated polymerase chain reaction (AL-PCR)

AL-PCR methodology was previously reported (30,41,48). Briefly, isolated total RNA was converted to double-stranded cDNA using the Superscript cDNA synthesis kit (Invitrogen, Carlsbad, CA), according to the manufacturer's instructions, except that a specific primer (BSL-18E) was used (48). The P10EA/P20EA adaptors were ligated to the 5′ end of cDNA and this adaptor-ligated cDNA was cut with *Sph* I. PCR was performed using TCR α-chain or β-chain constant region-specific primers (MCA1 or MCB1) and P20EA. The second PCR was performed with MCA2 or MCB2 and P20EA. Biotinylation of PCR products was performed using both P20EA and 5′-biotinylated MCA3 or MCB3 primers.

TCR repertoire analysis

TCRAV and TCRBV repertoires were analyzed using a microplate hybridization assay (MHA) (48). In brief, 10 pmol of amino-modified oligonucleotides specific for TCRAV and TCRBV segments were immobilized onto carboxylate-modified 96-well microplates with water-soluble carbodiimide. Prehybridization and hybridization were performed in GMCF buffer (0.5 M Na$_2$HPO$_4$, pH 7.0, 1 mM EDTA, 7% SDS, 1% BSA, and 7.5% formamide) at 47°C. One-hundred microliters of denatured 5′-biotinylated PCR products were mixed with an equivalent volume of 0.4 N NaOH/10 mM EDTA, and added to 10 mL of GMCF buffer. Hybridization solution (100 μL) was added to each well of the microplate containing immobilized oligonucleotide probes specific for the V segment. After hybridization, the wells were washed four times with washing buffer (2×SSC, 0.1% SDS) at room temperature. The plate was incubated at 37°C for 10 min for stringency washing. After washing four times with 2×SSC, 0.1% SDS, 200 μL of TB-TBS buffer (10 mM Tris-HCl, 0.5 M NaCl, pH 7.4, 0.5% Tween 20, and 0.5% blocking reagent; Boehringer Mannheim, Mannheim, Germany) were added to block non-specific binding. Next, 100 μL of 1:1000-diluted alkaline phosphatase-conjugated streptavidin in TB-TBS was added, and the sample was incubated at 37°C for 30 min. The plates were washed six times in T-TBS (10 mM Tris-HCl, 0.5 M NaCl, pH 7.4, and 0.5% Tween 20). For color development, 100 μL of substrate solution (4 mg/mL p-nitrophenylphosphate in 10% diethanolamine, pH 9.8) was added and the absorbance was determined at 405 nm. The ratio of the hybridization intensity for each TCRV-specific

probe to that of a TCRC-specific probe (V/C value) was determined using the TCR cDNA concentrated samples that contained the corresponding V segment and the universal C segment, respectively. Absorbances obtained for each TCRV-specific probe were divided by the corresponding V/C value. The relative frequency was calculated using the corrected absorbencies by the formula: relative frequency (%) = (corrected absorbance of TCRV-specific probe/the sum of corrected absorbencies of TCRV-specific probes)×100.

T-cell clonality analysis with CDR3 size spectratyping

PCR was performed for CDR3 size spectratyping (23) for 30 cycles in a $20 \mu L$ volume under the same conditions as described above. PCR assays used $1 \mu L$ of 1:20 or 1:50 diluted second PCR product, $0.1 \mu M$ of 5′-Cy5 MCA3/MCB3 primer, and $0.1 \mu M$ of the primer specific for each variable segment. Oligonucleotide probes for hybridization were used as primers specific for each variable segment (as described

above). Two microliters of 1:20-diluted PCR product in sample loading solution was analyzed using a CEQ8000 Genetic Analysis System (Beckman Coulter, Brea, CA). Spleen cells from mock-infected mice were used as a control for the peak patterns of peripheral blood.

Determination of nucleotide sequence of CDR3 regions

PCR was performed with $1 \mu L$ of 1:20 diluted second PCR product, using a forward primer specific to the variable region and a reverse primer specific to the constant region (MCA4 or MCB4) under the conditions described above. Primers VA8-1 (5′-ACGCCACTCTCCATAAGAGCA-3′), VA15-1 (5′-GTGGACAGAAAACAGAGCCAA-3′), and VB8-2 (5′-GGCTACCCCCTCTCAGACAT-3′) were used in this study. After elution from the agarose gel, PCR products were cloned into the pGEM-T Easy Vector (Promega Corp., Madison, WI). DH5α-competent cells were transformed with the
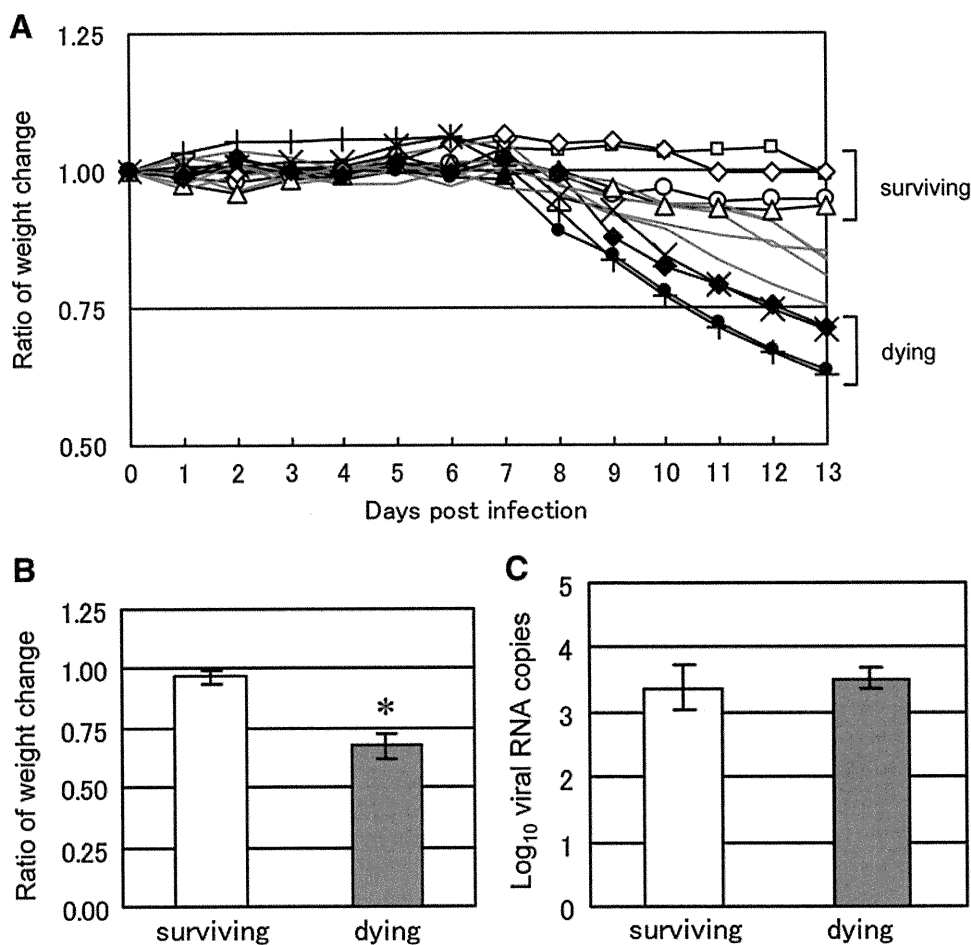

FIG. 1. Fatality of TBEV-infected mice is characterized by weight loss rather than brain viral replication. (**A**) Individual daily weight changes of TBEV-infected mice. Mice were monitored daily for signs of disease, and the ratio of weight change of individuals at each time point was compared with those at day 0 and recorded following subcutaneous infection with TBEV Oshima strain (10^3 PFU) in C57BL/6 mice (n = 13). Individuals with intermediate weight loss (10–25%) at 13 dpi are shown as gray lines, and mock-infected mice are not shown. (**B**) Average weight change ratios for surviving (ratio of weight change >0.90) and dying (<0.75) mouse groups at 13 dpi (n = 4). Error bars represent standard deviations. Asterisk indicates statistically significant ($p < 0.05$) differences between surviving and dying mice by Student's t-test. (**C**) Quantification of viral RNA in brains at 13 dpi. qPCR was performed using primers specific for TBEV NS1. Viral RNA copy number per 1 ng of total RNA is shown (n = 4). Statistically significant differences were not observed between surviving and dying mice.
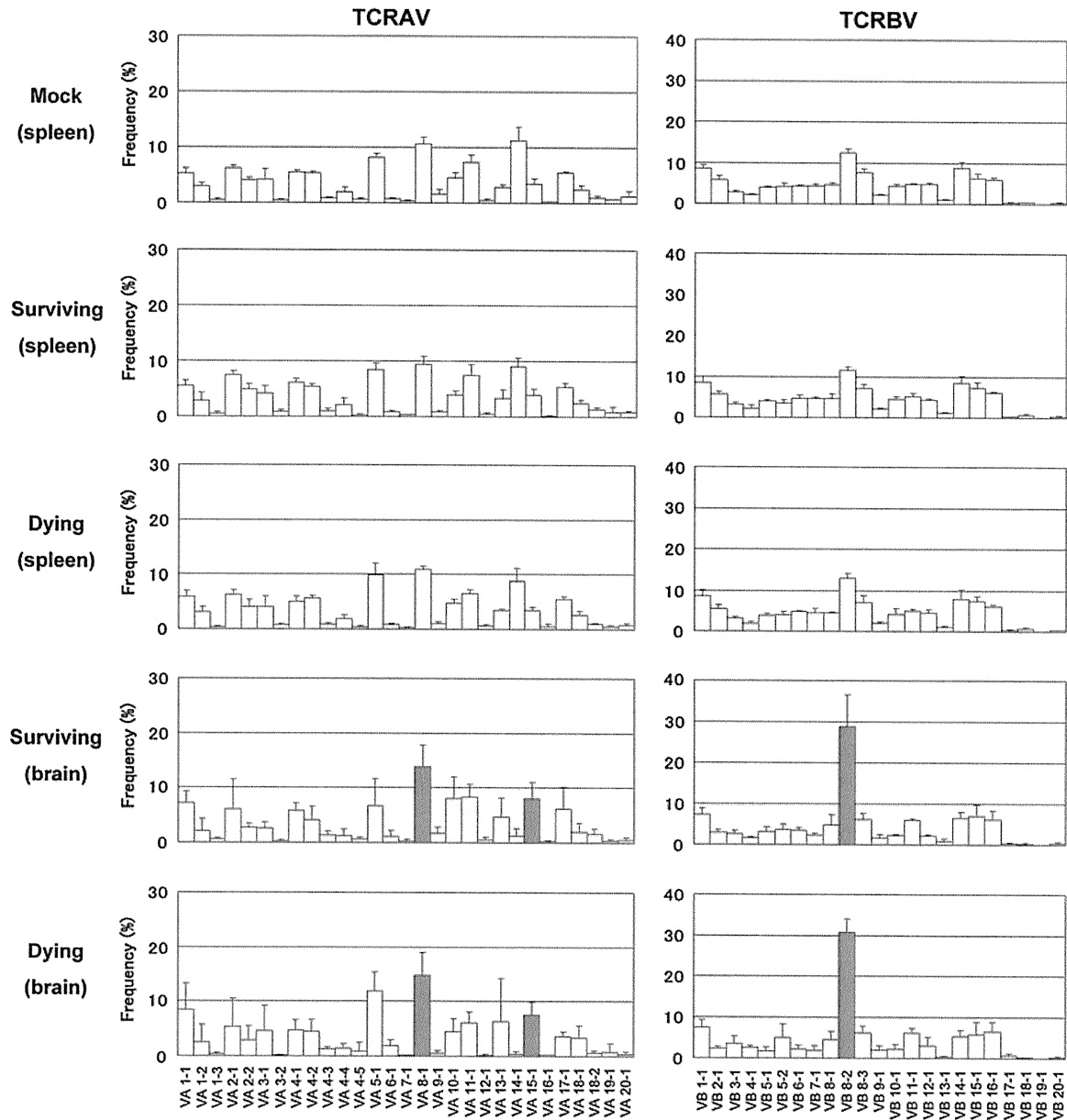
FIG. 2.   TCR repertoire analysis of spleens and brains from TBEV-infected or mock-infected mice. TCRAV and TCRBV repertoires were analyzed by MHA as described in the materials and methods section. Mean percent frequencies $\pm$ SD (standard deviation) of 4 mice are indicated. Gray bars indicate a significant increase compared with mock-infected spleens ($p < 0.05$ by Student's t-test).

recombinant plasmid DNA. Sequence reactions were performed with a GenomeLab DTCS Quick Start Kit (Beckman Coulter) and analyzed using the CEQ8000 Genetic Analysis System (Beckman Coulter).

Quantitative real-time PCR (qPCR)

mRNA expression levels of T-cell-related antigens, activation markers, and apoptosis-related genes for brains excised from TBEV-infected or mock-infected mice were determined by qPCR using a LightCycler (Roche Diagnostics Corp., Indianapolis, IN). Previously reported primer pairs specific for glyceraldehyde-3-phosphate dehydrogenase (GAPDH), CD3, CD4, and CD8 (10) were used in this study.

The following additional primer pairs were designed for our study: CD25 (forward: 5'-AAGATGAAGTGTGGGAAAA CGG-3', reverse: 5'-GGGAAGTCTGTGGTGGTTATGG-3'), CD69 (forward: 5'-AGGATCCATTCAAGTTTCTATCCC-3', reverse: 5'-CAACATGGTGGTCAGATGATTCC-3'), Granzyme (Gym) A (forward: 5'-CCTGAAGGAGGCTGT GAAAG-3', reverse: 5'-GAGTGAGCCCCAAGAATGAA-3'), Gym B (forward: 5'-CCATCGTCCCTAGAGCTGAG-3', reverse: 5'-TTGTGGAGAGGGCAAACTTC-3'), Perforin (forward: 5'- GCCTGGTACAAAAACCTCCA-3', reverse: 5'-AGGGCTGTAAGGACCGAGAT-3') and Fas ligand (FasL) (forward: 5'- GGGCAGTATTCAATCTTACCAG-3', reverse: 5'-GTGCCCATGATAAAGAATAGTAGA-3'). Freshly isolated RNA was converted to cDNA using a PrimeScript™ RT
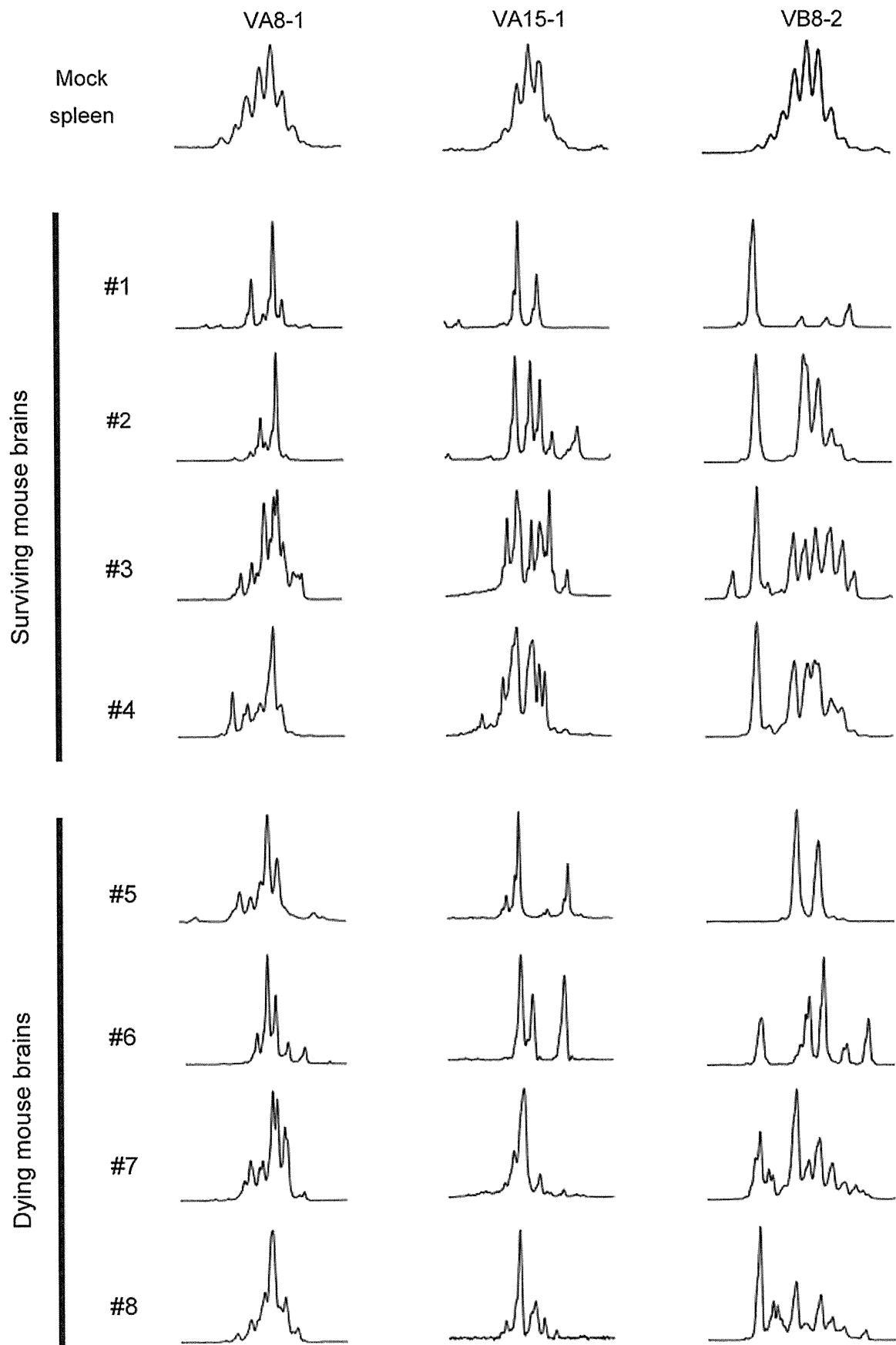
FIG. 3. CDR3 size spectratyping revealed different T-cell clonality patterns between surviving and dying mice. T-cell clonality for VA8-1, VA15-1, and VB8-2 families in individual mouse brains are shown. Peak numbers indicate the size variation of CDR3. Nucleotide size becomes longer at the right side. Generally, multiple peaks indicate the existence of polyclonal T cells, and one or a few peaks indicate the existence of monoclonal and oligoclonal T cells, respectively. Mock-infected spleen was used as a control to indicate polyclonal pattern.

A

AV8-1 (surviving mice)

mouse	freq.	V	N	J	J gene	
#1	3/12	CALS	DLVT	NTGKLTF	AJ27	[§]
	3/12	CALR	AHY	NQGKLIF	AJ23	†
	3/12	CALT	PNY	NQGKLIF	AJ23	[‡]
	1/12	CALS	PNY	NQGKLIF	AJ23	[†]
	1/12	CALR	PNY	NQGKLIF	AJ23	†
	1/12	CALG	PNY	NQGKLIF	AJ23	†
#2	8/11	CALS	HYQ	GGRALIF	AJ15	[*]
	3/11	CAL	KGS	SGNKLIF	AJ32	
#3	2/15	CALS	LAY	NQGKLIF	AJ23	†
	2/15	CALS	ASSS	GSWQLIF	AJ22	
	2/15	CALR	GQ	GGRALIF	AJ15	*
	2/15	CAL	KGY	NQGKLIF	AJ23	†
	1/15	CAC	KGY	NQGKLIF	AJ23	†
	1/15	CALS	EGY	NQGKLIF	AJ23	†
	1/15	CALS	PNY	NQGKLIF	AJ23	[†]
	1/15	CALT	PNY	NQGKLIF	AJ23	[‡]
	1/15	CALS	DLVT	NTGKLTF	AJ27	[§]
	1/15	CALS	GTSG	GNYKPTF	AJ6	
	1/15	CAL	IRGS	ALGRLHF	AJ18	
#4	6/13	CALS	HYQ	GGRALIF	AJ15	[*]
	3/13	CAL	W	MGYKLTF	AJ9	
	1/13	CALS	EPS	GSWQLIF	AJ22	
	1/13	CALS	VTG	SGGKLTF	AJ44	
	1/13	CAL	AGY	NQGKLIF	AJ23	†
	1/13	CA	ST	GYQNFYF	AJ49	

AV8-1 (dying mice)

mouse	freq.	V	N	J	J gene	
#5	5/11	CA	RN	SNNRIFF	AJ31	
	3/11	CALS	PNY	NQGKLIF	AJ23	[†]
	2/11	CALS	LN	YAQGLTF	AJ26	
	1/11	CA	STTA	SLGKLQF	AJ24	
#6	5/13	CALS	EGG	SNAKLTF	AJ42	
	5/13	CAL	YTE	GADRLTF	AJ45	
	2/13	CALS	GY	NQGKLIF	AJ23	†
	1/13	CALS	DHSYQ	GGRALIF	AJ15	
#7	3/15	CALS	DGG	TGSKLSF	AJ58	
	2/15	CALR	P	GYQNFYF	AJ49	
	2/15	CALS	PNY	NQGKLIF	AJ23	[†]
	1/15	CALS	QNY	NQGKLIF	AJ23	†
	1/15	CALS	Y	NQGKLIF	AJ23	†
	1/15	CALS	DGT	GGYKVVF	AJ12	
	1/15	CALS	GT	GGYKVVF	AJ12	
	1/15	CALS	VG	SNYQLIW	AJ33	
	1/15	CALR	LTSG	GNYKPTF	AJ6	
	1/15	CALS	DQTA	SLGKLQF	AJ24	
	1/15	CALR	SSYQ	GGRALIF	AJ15	
#8	3/12	CALS	ERN	YAQGLTF	AJ26	
	2/12	CALS	EGG	MGYKLTF	AJ9	
	2/12	CALR	RSP	GYQNFYF	AJ49	
	1/12	CAL	VNY	NQGKLIF	AJ23	†
	1/12	CAL	NTGG	LSGKLTF	AJ2	
	1/12	CALR	GS	AGNKLTF	AJ17	
	1/12	CA	ATS	SGQKLVF	AJ16	
	1/12	CA	WN	SNNRIFF	AJ31	

B

VA15-1 (surviving mice)

mouse	freq.	V	N	J	J gene	
#1	4/15	CAAS	MDY	NQGKLIF	AJ23	
	11/15	CAAG	N	AGAKLTF	AJ39	
#2	5/14	CAAS	TGA	NTGKLTF	AJ52	
	3/14	CAAK	EA	SNYQLIW	AJ33	[§]
	3/14	CAAS	IG	SNYQLIW	AJ33	
	2/14	CAAS	T	GYQNFYF	AJ49	
	1/14	CAAS	IWGA	NTGKLTF	AJ52	
#3	6/15	CAPG	GATA	SLGKLQF	AJ24	
	4/15	CAAT	N	YAQGLTF	AJ26	
	1/15	CAAS	WAS	GSWQLIF	AJ22	¶
	1/15	CAAS	WSS	GSWQLIF	AJ22	¶
	1/15	CAAS	TSS	GSWQLIF	AJ22	[¶]
	1/15	CAAS	S	NYNVLYF	AJ21	
	1/15	CAAG	T	GGYKVVF	AJ12	*
#4	10/14	CAAR	D	MGYKLTF	AJ9	[†]
	1/14	CAAS	P	MGYKLTF	AJ9	[‡]
	2/14	CAAK	EA	SNYQLIW	AJ33	[§]
	1/14	CAAS	TSS	GSWQLIF	AJ22	[¶]

VA15-1 (dying mice)

mouse	freq.	V	N	J	J gene	
#5	11/13	CAAR	T	GGYKVVF	AJ12	[x]
	2/13	CAAS	GA	GGYKVVF	AJ12	[*]
#6	5/10	CAAS	GA	GGYKVVF	AJ12	[*]
	5/10	CAAS	TSS	GSWQLIF	AJ22	[¶]
#7	5/13	CAAS	GA	GGYKVVF	AJ12	[*]
	4/13	CAAS	TA	GGYKVVF	AJ12	*
	3/13	CAAS	KA	GGYKVVF	AJ12	*
	1/13	CAAR	T	GGYKVVF	AJ12	[x]
#8	7/13	CAAR	D	MGYKLTF	AJ9	[†]
	2/13	CAAS	GA	GGYKVVF	AJ12	[*]
	1/13	CAAS	DGT	GGYKVVF	AJ12	*
	1/13	CAAS	P	MGYKLTF	AJ9	[‡]
	1/13	CAAS	TN	SGTYQRF	AJ13	
	1/13	CAAT	PPSS	GSWQLIF	AJ22	¶

FIG. 4. Amino acid sequences of TCR CDR3 regions of cDNA clones derived from TBEV-infected mouse brains. For the VA8-1 (**A**), VA15-1 (**B**) or VB8-2 (**C**) families, predicted amino acid sequences are shown with their frequencies of cDNA clones in each individual mouse. J gene usage is shown at the right side of each sequence. V, N (N-D-N), and J gene segments are not strictly divided. Each symbol indicates a group of identical or similar sequences, and brackets indicate an identical sequence among individuals.

C

VB8-2 (surviving mice)

mouse	freq.	V	N-D-N	J	J gene	
#1	8/17	CASGD		EQYF	BJ2.7	[*]
	4/17	CASSD	APPNTG	QLYF	BJ2.2	
	3/17	CASGD	LGGRGNYA	EQFF	BJ2.1	[§]
	1/17	CASRA	PWGEGTG	QLYF	BJ2.2	
	1/17	CASGD	ASFY	EQYF	BJ2.7	
#2	4/15	CASGD	ATGY	EQYF	BJ2.7	[¶]
	3/15	CASGE	LGAY	EQYF	BJ2.7	
	3/15	CASGD	MGQKD	TQYF	BJ2.5	[£]
	2/15	CASGD	AQLSY	EQYF	BJ2.7	
	2/15	CASGD		EQYF	BJ2.7	[*]
	1/15	CASGD	AGDRGV	EVFF	BJ1.1	
#3	2/10	CASGD	LGGRGNYA	EQFF	BJ2.1	[§]
	1/10	CASGD	LWGALNQD	TQYF	BJ2.5	
	1/10	CASGV	PGQGTTG	QLYF	BJ2.2	
	1/10	CASSG	QGAGNQ	APLF	BJ1.5	
	1/10	CASSD	ATISNE	RLFF	BJ1.4	
	1/10	CASGG	TGVAE	TLYF	BJ2.3	
	1/10	CASGE	GGVGN	TLYF	BJ1.3	
	1/10	CASGS	R	EQYF	BJ2.7	*
	1/10	CASGD		EQYF	BJ2.7	[*]
#4	2/10	CASGD	VRGDS	DYTF	BJ1.2	
	1/10	CASGD	MGQKD	TQYF	BJ2.5	[£]
	1/10	CASGK	LANQD	TQYF	BJ2.5	
	1/10	CANSE	WGADHD	TQYF	BJ2.5	
	1/10	CARGD	AGGSAE	TLYF	BJ2.3	
	1/10	CASKS	IQD	TQYF	BJ2.5	
	1/10	CASGD	ATGY	EQYF	BJ2.7	[¶]
	1/10	CASGD	G	GEYF	BJ2.7	*
	1/10	CASGD		EQYF	BJ2.7	[*]

VB8-2 (dying mice)

mouse	freq.	V	N-D-N	J	J gene	
#5	5/14	CASGT	PGGNT	EVFF	BJ1.1	
	3/14	CASGD	IRV	EVFF	BJ1.1	[†]
	3/14	CASGD	VRV	EVFF	BJ1.1	†
	2/14	CASGD	AWGKD	TQYF	BJ2.5	
	1/14	CASSD	APTSAE	TLYF	BJ2.3	
#6	8/13	CASGD	ATAIT	EVFF	BJ1.1	
	1/13	CASGG	DWGANTG	QLYF	BJ2.2	
	1/13	CASSD	LGVNYA	EQFF	BJ2.1	
	1/13	CASGD	NRV	EVFF	BJ1.1	[‡]
	1/13	CASGD		TQYF	BJ2.5	*
	1/13	CASGD		EQYF	BJ2.7	[*]
#7	2/13	CASGD	AGTG	EQYF	BJ2.7	
	2/13	CASGA	G	LGIF	BJ2.7	*
	1/13	CASGD	IRV	EVFF	BJ1.1	[†]
	1/13	CASGA	GST	EVFF	BJ1.1	†
	1/13	CASGG	GQKNS	DYTF	BJ1.2	
	1/13	CASGE	VGGRSA	EQFF	BJ2.1	
	1/13	CASGD	ALV	EQYF	BJ2.7	
	1/13	CASSD	AGW	EQYF	BJ2.7	
	1/13	CASGE		SEYF	BJ2.7	*
	1/13	CASGD		GPYF	BJ2.7	*
	1/13	CASGA		LEYF	BJ2.7	*
#8	3/15	CASGV	PY	EQYF	BJ2.7	
	2/15	CASGD		EQYF	BJ2.7	[*]
	1/15	CASGD	ARGNQD	TQYF	BJ2.5	
	1/15	CASGD	NRV	EVFF	BJ1.1	[‡]
	1/15	CASGE	AW	GGAF	BJ2.5	
	1/15	CASGD	AGHSY	EQYF	BJ2.7	
	1/15	CASGD	LGAD	EQYF	BJ2.7	
	1/15	CASGD	G	GEYF	BJ2.7	*
	1/15	CASGD		FQYF	BJ2.7	*
	1/15	CASGD		TLYF	BJ1.3	
	1/15	CASGD		EVFF	BJ1.1	

FIG. 4.   (Continued).

reagent kit (Takara Bio Inc., Shiga, Japan), and the PCR reaction was performed using SYBR® Premix Taq™ (Takara Bio) for SYBR Green I according to the manufacturer's instructions. The expression level of each gene was measured by qPCR as demonstrated previously (10). Expression levels were normalized based on the housekeeping gene GAPDH copy number. Relative quantification was expressed as a ratio between TBEV-infected and mock-infected brains.

Viral RNA levels of TBEV were examined with NS1-specific primers (forward: 5′-CGGCTAGCCACACTATCGA CAA-3′, reverse: 5′-GGCGAGTACTTCCATGGTCCTT-3′). Reverse transcription and PCR reactions were conducted as described above. Viral RNA was quantified as copy number per 1 ng of total RNA. Copy number in each sample was determined on the basis of a standard curve.

Statistical analysis

Student's *t*-test was used for statistical analysis to assess significant differences in weight change ratio, the degree of the relative expression in TCR repertoire analysis, and the expression levels of genes in qPCR analysis. The Mann-Whitney *U* test was used to evaluate frequencies of CDR3 sequences. A *p* value <0.05 was determined to be statistically significant.

Results

Discrimination of surviving and dying mice

Thirteen C57BL/6 mice were subcutaneously inoculated with 10^3 PFU of TBEV and weighed daily (Fig. 1A). Four mice from each of the surviving and dying groups were used in the experiments. Dying mice were defined as those exhibiting more than 25% weight loss at 13 dpi, and surviving mice were defined as those with less than 10% weight change. Mock-infected mice (n = 4) exhibited negligible weight change (data not shown). Weight percentage at 13 dpi, compared with that on day 0, was significantly different between the surviving and dying mouse groups (Fig. 1B). However, the amounts of viral RNA in the brains at the 13 dpi were no different between these two groups of mice (Fig. 1C). These data indicate that the virus propagation level is not the main factor that determines the fatality of TBEV-infected mice.

TCR repertoire analysis

TCRAV and TCRBV repertoires were analyzed using brains and spleens collected from TBEV-infected dying mice, surviving mice, or mock-infected mice at 13 dpi (Fig. 2). Using TCR repertoire analysis, significant expressions of TCRAV and TCRBV were detected in TBEV-infected brains

◄F1

◄F2

both in surviving and dying mice. Frequencies of T cells bearing VA8-1, VA15-1, and VB8-2 were significantly increased in brains compared with mock-infected spleens. However, there was no significant difference between surviving and dying mice. VA14-1, known as the family expressed on NKT cells (3), was expressed at very low levels in virus-infected brains. No difference between mock-infected and TBEV-infected mouse spleens was observed for both TCRAV and TCRBV repertoires, and this suggests that systemic T-cell response changes were below the detectable level in our analysis. In mock-infected mouse brains, the expression of TCRAV and TCRBV was not detected (data not shown) due to the low lymphocyte numbers.

CDR3 size spectratyping

We performed CDR3 size spectratyping analysis to confirm the clonalities of T cells expressing VA8-1, VA15-1, and F3 ▶ VB8-2 families in TBEV-infected mouse brains (Fig. 3). Different patterns were observed between TBEV-infected brains and mock spleens for all three families. Furthermore, VA15-1 clonalities for dying mice were higher than those for surviving mice. A short VB8-2 size peak was also observed in surviving mice.

Amino acid sequences of CDR3

Because differences in T-cell clonality were observed between surviving and dying mice, nucleotide sequences of the CDR3 were determined for the above-mentioned TCR families, using PCR-amplified and randomly-selected cDNA clones. Predicted amino acid sequences are shown along with the frequencies of cDNA clones derived from the F4 ▶ brains of individual mice infected with TBEV (Fig. 4). Cysteine (C) at the N-terminal portion and phenylalanine (F) or tryptophan (W) at the C-terminal portion are not contained within CDR3. Despite the fact that we analyzed more than 30 clones in mock-infected spleens, we did not find any clones with identical sequence (data not shown). Meanwhile, in TBEV-infected brains, many clones with identical sequences were found. VA8-1 (Fig. 4A) surviving mice were divided into two groups: individuals with high frequency of AJ23 gene usage (#1 and #3) or AJ15 gene usage (#2 and #4). Although dying mice also produced some clones bearing AJ23 or AJ15, the frequency of these clones was lower than in surviving mice. For VA15-1 (Fig. 4B), a high frequency of AJ12 gene usage was observed in dying mice. In addition, clones with identical amino acid sequences to CDR3 (CAAS GA GGYKVVF) were detected in all four dying mice. Identical clones bearing AJ9 and AJ22 were detected in both surviving and dying mice. For VB8-2 (Fig. 4C), a high frequency of BJ2.7 genes with short CDR3 consisting of seven amino acids (aa) was characteristic for both surviving and dying mice. Clones with such a short CDR3 were rare in TCR β chains. Some clones bearing BJ1.1 with 10 aa CDR3 (CASGD XRV EVFF, X = I, V or N) were found in every dying mouse. As shown for VA8-1, VB8-2 surviving mice were also divided into two groups: individuals (#1 and #3) that obtained clones with BJ2.1 (CASGD LGGRGNYA EQFF), or individuals (#2 and #4) that obtained clones with BJ2.7 (CASGD ATGY EQYF) and BJ2.5 (CASGD MGQKD TQYF). The frequencies of these three clones were not high in each individual, but were specific

for each group. In mouse #5, there was no clone bearing BJ2.7 or short CDR3, therefore the frequency of these clones might be high but not necessary in TBEV-infected mice. As illustrated by mice #7 and #8, a high single peak in CDR3 size spectratyping analysis does not necessarily indicate monoclonal expansion. Clones were also sometimes included that were the same size as CDR3, yet had different sequences. However, several reports have shown that the β-chain J region of CDR3 does not specifically interact with antigen peptides (7,11,13,14,43). The sequence of the N-terminal half of CDR3 (V segment, D segment, and N addition) rather than J gene usage might therefore be important, as potentially each clone with a short CDR3 recognizes an identical antigen peptide. To organize sequence data, clone frequencies with more than 10% J gene usage in the total number of clones analyzed for each V family were individually plotted in Fig. 5. CDR3 length was ◀ F5 considered for the β chain. Using the Mann-Whitney U test, the frequency of VA8-1/AJ15 was significantly higher in surviving mice, and the frequencies of VA15-1/AJ12 and VB8-2/BJ1.1 (10 aa) were significantly higher in dying mice. This suggests that these T-cell clones might be closely associated with disease severity in TBEV-infected mice.

Levels of cell surface markers and cytokines determined by qPCR

Differential patterns of T-cell clones can indicate that brain-infiltrating cells may play different roles between surviving and dying mice. To investigate the active state of the infiltrating cells, we studied the expression levels of T-cell antigen markers, lymphocyte activation markers, and apoptosis-related genes: CD3, CD4, CD8, and CD25 (expressed on activated T cells and B cells) (28), CD69 (expressed rapidly after lymphocyte activation) (47), and Gzm A, Gzm B, perforin, and FasL using qPCR analysis (Fig. 6). ◀ F6 The resulting expression levels for all genes in TBEV-infected brains studied were significantly increased when compared with mock infection. This was especially the case for the expression of CD69, Gzm A, and Gzm B, which were increased more than 100 times. No significant differences were observed between mouse groups, indicating that equivalent $CD8^+$ T-cell infiltration into TBEV-infected brains occurs in surviving and dying mice with similar activation state levels.

Discussion

Understanding the clinical variability caused by encephalitic flavivirus infection is important in explaining differences between severe and subclinical human cases. It may also further elucidate the mechanism of pathogenesis for viral encephalitis. Previous reports showed that the TBEV Oshima strain elicited dose-independent mortality following peripheral infection in some mouse strains (6,21). We therefore distinguished surviving and dying mice by their degree of weight loss after TBEV infection according to our previous study (21), as a simple and effective method to evaluate the severity.

Based on the amount of viral RNA in brain tissue, we found no difference in virus replication between surviving and dying mice. This result suggests that direct virus-induced neuronal injury cannot completely explain the